Ulm University
Department for Internal Medicine I
Head of Department: Prof. Dr. med. Thomas Seufferlein

Role of Protein Kinase D1 in pancreatic cancerogenesis

Dissertation submitted to obtain the doctoral degree of
'Doctor of medicine' (Dr. med.) of the Medical Faculty of the University of Ulm

by
Yasin Bektas, born in Weingarten
submitted in 2019

Acting Dean:	Prof. Dr. rer. nat. Thomas Wirth
1st reviewer:	Prof. Dr. med. Thomas Seufferlein
2nd reviewer:	Prof. Dr. med. Dr. hc. Matthias Tisch
Date of graduation:	12.04.2021

Table of Contents I

Abbreviations II

1. Introduction 1

1.1 Pancreatic Cancer 1

1.2 Development and Progression of Pancreatic Ductal Adenocarcinoma 1

1.3 Inflammation in PDAC Development 3

1.4 Recent and Potential Therapy of Pancreatic Cancer 5

1.5 The Serine-Threonine Protein Kinase D 6

1.5.1 Structure 6

1.5.2 PKD Function PKD1 6

1.6 Murine Model of PDAC Development 8

1.7 Aim of the study 9

2. Material and Methods 10

2.1 Material 10

2.1.1 Buffers and Solutions 10

2.2 Methods 11

2.2.1 Tissue processing for immunohistochemistry 11

2.2.2 Stainings 11

3. Results 14

3.1 Generating the P48-Cre-KRAS^{G12D}-PKD1$^{-/-}$ Mouse Model 14

3.2 Pancreas specific knockout of PKD1 decreases survival 15

3.3 Histo-pathological examination revealed a significant Tumor progression in *P48-Cre-KRAS^{G12D}-PKD1$^{-/-}$* mice 16

3.4 Progression of the precancerous lesions to pancreatic cancer is accompanied by development of rich desmoplastic reaction in p48-Cre-KRAS^{G12D}-PKD1$^{-/-}$mice 19

3.5 Increasing influx of leukocytes during PDAC progression 21

4. Discussion 35

5. Summary 41

6. References 42

Acknowledgments 49

Curriculum Vitae **Fehler! Textmarke nicht definiert.**

Abbreviations

ADM	Acinar-to-ductal metaplasia
CAM	Chorioallantois membrane
CCK	Cholecystokinin
CK19	Cytokeratin-19
COX2	Cyclooxygenase 2
ddH_2O	Double-distilled water
dH_2O	Distilled water
ECM	Extracellular matrix
EDTA	Ethylenediamine tetraacetic acid
EtOH	Ethanol
GEMM	Genetically engineered mouse model
H&E	Hematoxylin and eosin
HIER	Heat-induced epitope retrieval
IFN	Interferon
IHC	Immunohistochemistry
IL	Interleukin
IPMN	Intraductal papillary mucinous neoplasms
$KRAS^{G12D}$	p48-Cre-$KRAS^{G12D}$
$KRAS^{G12D}$-$PKD1^{-/-}$	p48-Cre-$KRAS^{G12D}$-$PKD1^{-/-}$
MCN	Mucinous cystic neoplasms
MDSC	Myeloid-derived Suppressor Cell
MMP	Matrix metalloproteinase
NF-κB	Nuclear factor kappa-light-chain-enhancer of activated B cells
NK cells	Natural killer cells
PanIN	Pancreatic intraepithelial neoplasia
PBS	Phosphate-buffered saline
PDAC	Pancreatic ductal adenocarcinoma

PKD	Protein Kinase D
$PKD^{-/-}$	p48-Cre-$PKD1^{-/-}$
PSC	Pancreatic stellate cell
SEM	Standard error of the mean
TAM	Tumor-associated macrophages
TBS-T	Tris-buffered saline TWEEN
TNF	Tumor necrosis factor
T_{reg}	Regulatory T-Lymphocytes
TRIS	Tris(hydroxymethyl)aminomethane
VEGF	Vascular endothelial growth factor

1. Introduction

1.1 Pancreatic Cancer

Pancreatic cancer is the fourth leading cause of cancer death preceded by lung, colon and breast/prostate cancer (Siegel *et al.* 2017). Approximately 17,000 people were diagnosed with pancreatic cancer in Germany in 2014 (www.krebsdaten.de). It has a dismal 5-year survival rate of 5% due to the lack of symptoms in early stages and detection at the later already metastatic stages (Jemal 2017). Potential risk factor for developing pancreatic cancer are genetic predispositions, such as mutations in *BRCA2, CDKN2A, PRSS1, STK11* and *PALB2* gene loci (Grant *et al.* 2015). Furthermore, recent analyses indicate a positive correlation between inflammation and pancreatic cancer, especially chronic pancreatitis is responsible for pancreatic ductal adenocarcinoma in adult mice (Seimiya *et al.* 2018; Guerra *et al.* 2007). Various studies have identified three different types of potential precursor lesions for pancreatic cancer (Ren *et al.* 2019). These include intraductal papillary mucinous neoplasms (IPMN), which arise in main pancreatic ducts or their major branches, mucinous cystic neoplasms (MCN) and Pancreatic Intraepithelial Neoplasia (PanIN) lesions which are assumed to originate from transdifferentiation of acinar cells (Ren *et al.* 2019). The majority of pancreatic cancer types are adenocarcinomas of the exocrine pancreas which are arise very likely from PanINs (Ren *et al.* 2019).

1.2 Development and Progression of Pancreatic Ductal Adenocarcinoma

Pancreatic ductal adenocarcinoma accounts for almost 90% of all malignant pancreatic neoplasms which have been shown to develop through different precursor lesion stages, characterized by morphologic and genetic changes (Ren *et al.* 2019; Vincent *et al.* 2011). These changes are often a result from a series of mutations in various proto-oncogenes and tumor-suppressor genes. The most prevalent and significant proto-oncogene in pancreatic cancer is *KRAS* (Kamisawa *et al.* 2016). Together with additional tissue damage, these genetic alterations lead to metaplasia of acinar cells (acinar-to-ductal metaplasia [ADM]) (He et al. 2018). ADMs are precursors of PanIN lesions and were shown to arise from acinar cells (He et al. 2018). This transdifferentiation is caused by acinar injury, induced by pancreatic inflammation (pancreatitis), epidermal growth factor receptor activation, and by a mutated *KRAS* proto-oncogene (He *et al.* 2018; Kirkegard *et al.* 2017). Further progression of those PanIN lesions lead to pancreatic cancer (Yamaguchi et al. 2018). PanIN are classified in three grades; PanIN-1, PanIN-2, and PanIN-3. In order from least severe to most severe, based on the degree of dysplasia, whereby the last stage is already a carcinoma-in-situ (Distler *et al.* 2014).

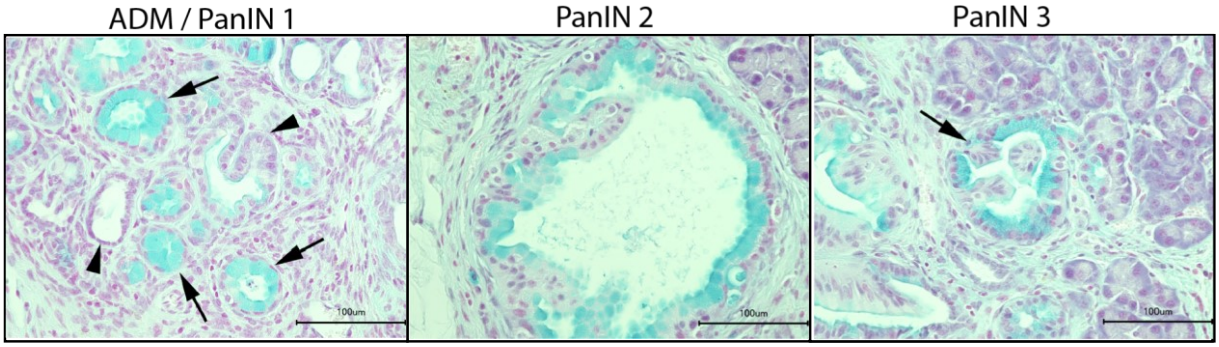

Figure 1: Classification of PanIN lesions based on Basturk et al. 2015

Figure shows ADMs (arrowhead) and PanIN lesions (arrows). Blue mucin content is the characteristic feature of PanINs which is used to differentiate between ADM and PanIN Size bars indicate 100 µm.

PanIN: *Pancreatic intraepithelial neoplasia;* ***ADM:*** *Acinar-to-ductal metaplasia*

Normal pancreatic ductal cells show cuboidal and low columnar epithelium absent of mucinous cytoplasm (Basturk *et al.* 2015). PanIN-1 lesions are tall columnar cells, basally located nuclei, and supranuclear mucin, whereas PanIN-2 lesions display nuclear abnormalities and can be flat or papillary (Basturk *et al.* 2015). Characteristic of PanIN-3 lesions are their papillary or micropapillary architecture and the appearance of small clusters of epithelial cells budding off into the lumen (Basturk *et al.* 2015).

Pro oncogenic *KRAS* mutation is found in more than 90% of cancer cases and can already be detected in the early PanIN-1 formations with a progressive increase correlating to PanIN levels (Biankin *et al.* 2012; He *et al.* 2018). KRAS mutations have also been detected in 30% of chronic pancreatitis patients, a condition that is a known risk factor for PDAC (Kamisawa *et al.* 2016). Other alterations in early disease stage include overexpressed ERBB2 and EGFR (Kamisawa *et al.* 2016).

PDAC development is accompanied by a desmoplastic reaction, comprised of cellular components such as fibroblasts, stellate cells, immune cells, and non-cellular multiple extracellular matrix (ECM) proteins (Ahrens *et al.* 2017). This reaction starts much earlier than an actual carcinoma occurs and is frequently observed around PanINs in very early stages of disease (Ahrens *et al.* 2017). It is also known as a resistance factor to chemotherapy/radiation therapy and a drug delivery barrier (Neesse *et al.* 2011). One of the most important stromal components are the pancreatic stellate cells (PSC). PSC actively proliferate, migrate, and produce ECM proteins, including type I and III collagen, laminin and fibronectin (Habisch *et al.* 2010; Ohlund *et al.* 2017). Additionally, activated PSCs secrete metallo-proteases, cytokines and growth factors which stimulate cancer cells to proliferate, migrate and invade local and

distant organs (Wehr *et al.* 2011). Taken together, all these effects of PSCs lead them to be considered a main source of stroma production and an important factor to cancer promotion and sustain.

Inflammatory cells are another crucial cell population in stromal tissue of PDAC (Clark *et al.* 2007). Clark *et al.* have shown that infiltrating immune cells are mainly composed of myeloid-derived suppressor cells (MDSC), regulatory T-lymphocytes (T_{reg}), and tumor-associated immunosuppressive macrophages (TAM) (Banerjee *et al.* 2018; Clark *et al.* 2007). An increased number of $CD8^+$ and natural killer cells are associated with better prognosis and are less frequently seen in pancreatic cancer (Banerjee *et al.* 2018; Clark *et al.* 2007). It is assumed that an early infiltration of immune suppressing cells (MDSC, TAM and T_{reg}) as well as the stromal microenvironment are responsible for permitting anti-tumorigenic reaction by subduing effector T cell attraction, activation and their access to tumor cells (Banerjee *et al.* 2018; Clark *et al.* 2007).

1.3 Inflammation in PDAC Development

In various organs, inflammation is often associated with neoplastic changes, and pancreatic cancer is no exception (Banerjee *et al.* 2018; Clark *et al.* 2007). Chronic and recurrent inflammations of the pancreas is highly associated with PDAC. COX-2, an inflammatory enzyme, has been reported to be elevated in human pancreatic cancer and PanINs lesions (Pomianowska *et al.* 2014). These results indicated a strong correlation between inflammation and pancreatic cancer. It has been predicted as an important possible target for pancreatic cancer treatment (Pomianowska *et al.* 2014). The inhibition of COX-2 by celecoxib resulted in reduced tumor growth in pancreatic cancer, but it has not been clearly identified how COX-2 is regulated during PDAC progression (Pomianowska *et al.* 2014).

The initiation and maintenance of inflammation with accompanied immunosuppression are caused through different types of leukocytes of innate and adaptive immune cells, including normal and tumor-associated macrophages, neutrophils, dendritic cells, mast cells and lymphocytes (Zhang *et al.* 2017; Liou *et al.* 2013; Greer *et al.* 2013). Clark *et al.* characterized the pancreas infiltrating immune cells at different stages of normal and tumorous pancreata using a mouse model that mimics human pancreatic cancer through induction of the oncogenic *KRAS* gene (Melstrom *et al.* 2017; Clark *et al.* 2007). Tumor-associated-macrophages, MDSC and regulatory T-lymphocytes are observed in early stages of disease with PanIN lesions (Melstrom *et al.* 2017; Clark *et al.* 2007). Macrophages are a dominating and important cell type and persist throughout progression from PanIN lesions until PDAC development (Clark *et*

al. 2007; Melstrom *et al.* 2017). Tumor-associated macrophages (TAM) mostly promote tumor development and metastasis by its function as an ECM producing and degrading cell type. By remodelling the environmental stroma through releasing MMPs and collagens, they seem to facilitate cell migration within the tumor (Ostrand-Rosenberg *et al.* 2012; Ruffell, Affara and Coussens 2012). Macrophages are distinguished by their function as either M1 and M2 macrophages, whereby the M1 subtype is more anti-tumorigenic and M2 macrophages have tumor-promoting features (Ruffell, Affara and Coussens 2012; Ostrand-Rosenberg et al. 2012). $CD8^+$ cells are responsible for killing cells expressing a foreign antigen and for tumor surveillance (Melstrom *et al.* 2017). Unfortunately, these $CD8^+$ T-lymphocytes are scarcely seen in PDAC (Melstrom *et al.* 2017; Clark *et al.* 2007). This phenomenon is assumed to be associated with MDSC domination, inverse correlation between the prevalence of MDSC and the prevalence of $CD8^+$ T cells (Melstrom *et al.* 2017; Clark *et al.* 2007). An anti-tumor activity and a significantly positive clinical outcome in pancreatic cancer with increased $CD8^+$ cells infiltration has been shown (Melstrom *et al.* 2017). $CD4^+$ T-cells can differentiate into Th_1, Th_2, and T_{reg} subpopulations and have various functions (Luheshi *et al.* 2014). Th_1 cells produce several cytokines such as IL-2, TNF-α, and IFN-γ, which lead to T-cell proliferation, activation and differentiation of macrophages as well as inhibition of Th_2 cells (Luheshi *et al.* 2014). Th_2 cells, in contrast, were assumed to have pro-tumorigenic effects with tumor-promoting function as well as with reduced survival of patients with pancreatic cancer (De Monte *et al.* 2016). Other tumor supporting cells are regulatory T-cells (T_{reg}) cells. T_{reg} cells are important for immunological self-tolerance. They are assumed to impair the anti-tumor immune response in various cancer types (Joshi *et al.* 2015). Increased T_{reg} cells were found in peripheral blood and in the microenvironment of patients with pancreatic cancer (Jang *et al.* 2017; Clark *et al.* 2007). It is also known that T_{reg} cell infiltration correlates with progression of pre-neoplastic lesions and metastasis. This T_{reg} cell infiltration also negatively correlates with patient survival rate (Jang *et al.* 2017; Tang *et al.* 2014). T_{reg} cells inhibit IL-2 production, promote cell-cycle arrest in $CD4^+$ and $CD8^+$ T-cells and lead to a decreased CD8 activation (Jang *et al.* 2017).

CD40 is a membrane glycoprotein member of the TNF receptor family and it is present on various cell populations including dendritic cells, monocytes and B lymphocytes (Beatty *et al.* 2011). It is considered as a potential therapeutic target in recent years (Jang *et al.* 2017). Activation of $CD40^+$ cells drives a T- and dendritic cell response and leads to a tumor suppressive microenvironment (Beatty *et al.* 2011; Jang *et al.* 2017). CD40 activation also promotes pro-inflammatory cytokines, that result in an anti-tumor response. Beatty et al. aimed to suppress T-cell promoted progression by using CD40 antibodies and the result showed a

tumor regression by reprogramming of M2 TAMs into anti-tumor M1 TAMs (Beatty *et al.* 2011; Jang *et al.* 2017).

1.4 Recent and Potential Therapy of Pancreatic Cancer

Surgical resection is currently the only curative therapeutic strategy for pancreatic cancer (Muranaka *et al.* 2017). A late stage disease with metastasis is treated with Folforinox protocols and a combination of gemcitabine and nanoparticle albumin-bound paclitaxel (Muranaka *et al.* 2017). Various colorectal carcinomas are already treated with targeted therapies, but there are no comparable therapy strategies for pancreatic cancer, with the exception of tyrosine kinase inhibitor erlotinib in combination with gemcitabine (Hammel *et al.* 2016). A dismal 5-year survival rate shows the need for more therapeutic strategies (Hammel *et al.* 2016). In recent years, there has been important progress in understanding the biology and molecular mechanism of pancreatic cancer development, but still no proper targeted therapy options were available (Hammel *et al.* 2016). It has been shown in pancreatic cancer cells, that increased *PKD1* level increases the invasiveness of PDAC (Ochi *et al.* 2011). Recent studies have revealed the serine-threonine family PKD (Protein Kinase D) as a possible therapeutic target for PDACs (Harikumar *et al.* 2010). The first orally bioavailable and tumor growth-blocking agent was found by Guha *et al.* (Harikumar *et al.* 2010, Guha *et al.* 2010). They used a tumor model, that was treated with a PKD inhibitor. It increased cell apoptosis and significantly abrogated pancreatic cancer growth (Harikumar *et al.* 2010). These results encourage further investigations regarding *PKD1* and its possible uses as a potential therapeutic target. Hence, we decided to investigate the role for *PKD1* in PDAC in a mouse model.

1.5 The Serine-Threonine Protein Kinase D

1.5.1 Structure

The PKD family is a serine-threonine kinase that is comprised of *PKD1*, *PKD2* and *PKD3* which play important roles in different biological cell functions and various diseases (Roy *et al.* 2017). The important structural characteristics of the PKD family are the C-terminal catalytic domain and the N-terminal regulatory domain. All three isoforms contain a cystein-rich domain with two Zinc-finger like structures (C1a and C1b) and a pleckstrin homology domain (PH) (Roy *et al.* 2017). The N-terminal domains of *PKD1* and *PKD2* are known as the negative kinase activity domain, as well as the PH domain. The deletion of those regions results in an increased activity of *PKD1* and 2, whereas the C1a and C1b regions in *PKD2* seem to be acting as a stimulator of the kinase activity (Roy *et al.* 2017).

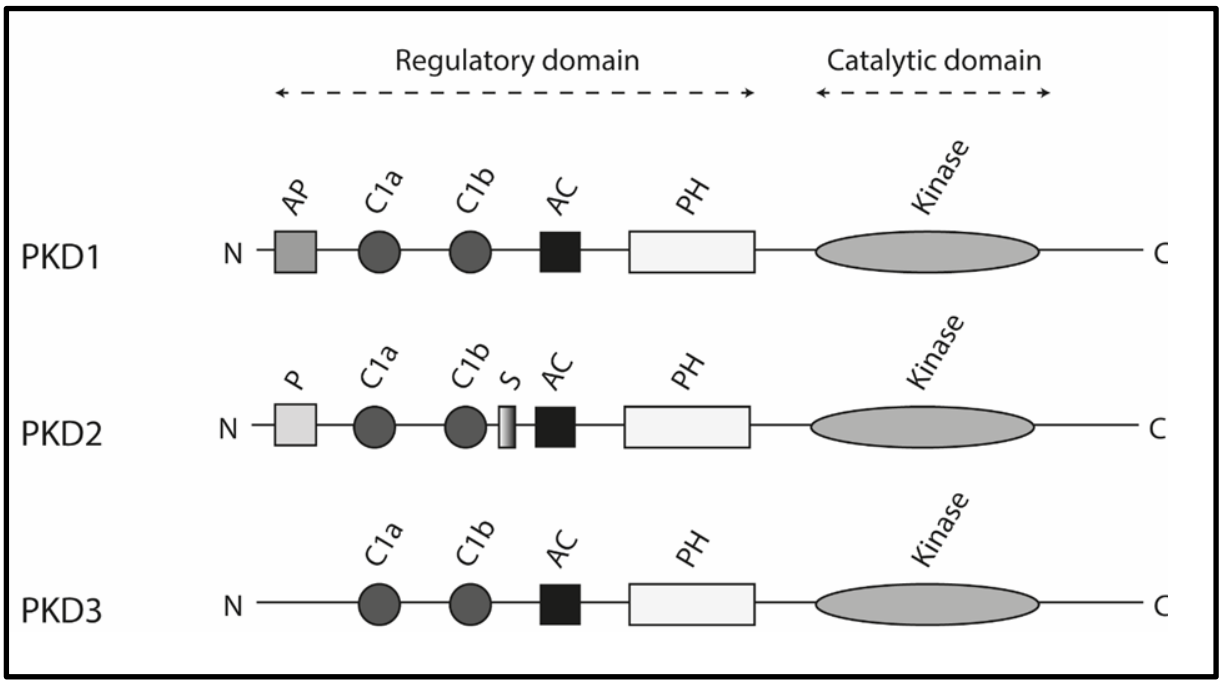

Figure 2: PKD family

Graph shows the molecular structure of the PKD-Family. All three isoforms contain a N-terminal regulatory domain, a zinc finger-like cysteine-rich domain (called CIa and CIb), a plekstrin homology (PH) domain and a C-terminal catalytic domain.
AP: *alanin-/proline-rich domain;* ***C:*** *COOH-terminus;* ***C1a/C1b:*** *cysteine-rich domain;* ***N:*** *NH2-terminus;* ***P:*** *proline-rich domain;* ***S:*** *serine-rich domain;* ***AC:*** *acidic domain;* ***PH:*** *pleckstrin homology domain; (Figure based on Roy et al. 2017)*

1.5.2 PKD Function PKD1

PKD1 is the most studied member of the family and is associated with various cancer development processes by regulating different cell functions such as cell proliferation, cell motility, cell polarity, angiogenesis and inflammation (Guha *et al.* 2010).

Dysregulation in cell proliferation and apoptosis are main characteristics of cancer initiation and progression, including pancreatic cancer (Harikumar *et al.* 2010). Cytokines, such as tumor necrosis factor α (TNFα), an important contributor to PDAC as an apoptosis initiator, can be affected in its function by overexpressed *PKD1*, leading to an inhibition of the apoptosis process in cells (Harikumar *et al.* 2010). Furthermore, the activation of NF-κB as a response to oxidative stress-induced cell death, is also mediated by *PKD* (Harikumar *et al.* 2010). Activation is induced by phosphorylation at the PH domain by the Src and Abl tyrosine kinases and activates in turn the NF-κB pathway via IKK beta (Harikumar *et al.* 2010). This reaction induces an inflammatory response and prevents the cells from apoptosis (Harikumar *et al.* 2010). Invasion by degradation of extracellular matrix and basal membranes by matrix metalloproteinases is a crucial step in tumor spreading (Eisler *et al.* 2009). Previous studies have shown contrasting effects of *PKD1* in cell migration and tumor cell invasion (Eisler *et al.* 2009). For breast and prostate cancer there have been shown a decreasing cell invasiveness potential for *PKD1* signalling, whereas other research groups have revealed the tumor growth prevention effect of *PKD1*-inhibitors (Eiseler *et al.* 2009; Harikumar *et al.* 2010, 2010; Peterburs *et al.* 2009). It appears that its exact influence depends on context of activation. In pancreatic cancer cells, it has been shown that increased *PKD1* level increases the invasiveness of PDAC (Ochi *et al.* 2011). Further studies have affirmed the effect of preventing tumor invasiveness by *PKD1* (Eiseler *et al.* 2012). They have revealed that *PKD1* knockdown lead to enhanced tumor cell invasion but has an inhibitory effect on cell proliferation (Eiseler *et al.* 2012). So, they proposed an anti-invasiveness and pro-proliferative feature for *PKD1*, whereas the *PKD2* isoform is considered to be a tumor invasiveness promoting protein (Wille, Seufferlein and Eiseler 2014). Tumor invasion also requires the ability to degrade ECM, especially by secreting MMPs (Wille *et al.* 2014). This part is mostly taken over by *PKD2* and its ability to enhance MMP7/9 secretion (Wille *et al.* 2014). MMP-7 and -9 are shown to regulate tumor invasiveness, especially enhancement of pancreatic cancer cell invasiveness in 3D-ECM fibroblast overlay invasion, and CAM (chorioallantois membrane) models (Wille *et al.* 2014). In the same study, MMP9 regulates and enhance PKD2-mediated tumor angiogenesis by regulating VEGF-A secretion and therefore its effects of tumor vascularization and growth, which is a known, important factor for various cancer types (Wille *et al.* 2014). It has been described that *PKD1* can be activated in PDAC by oncogenic KRAS (Liou *et al.* 2015). This stimulation leads to activation of NF-κB and its downstream pathways, that activate inflammatory reactions and may lead to ADM formations and upregulation of inflammatory cytokines (Liou *et al.* 2013). Previous data has suggested that *PKD1* expression is comparably low in many PDACs whereas

PKD-2 is up-regulated in PDAC, which lead to further investigations in order to assess their possibilities for a therapeutic target (Azoitei *et al.* 2010; Porzner and Seufferlein 2011, Wille *et al.* 2014). Those results lead to further studies about *PKD1* inhibitors as a potential therapy, but there is still need for more investigations in order to find an effective therapeutic agent.

1.6 Murine Model of PDAC Development

Before development of genetically engineered mouse models (GEMMs) of pancreatic cancer, tumor transplantation models were used to assess cancer cells in mouse models (Kim *et. al*. 2009). Human pancreatic tumor cell lines were implanted in mice and further investigations were made to acquire information about tumor growth and behaviour (Kim *et. al*. 2009). These models however, do not recapitulate the development and induction of immune tolerance that occurs in human pancreatic cancer. An implantation leads to immune activation and alterations of the tumor microenvironment, so that there was a need for another investigation model, the GEMMs. GEMMs spontaneously develop PanINs and pancreatic cancer in the context of a competent and intact immune system (Hingorani *et al.* 2005; Beatty *et al.* 2011). GEMMs are suitable to study pancreatic cancer from its initiation to fully developed tumor in a microenvironment that is not affected by immune reactions to implanted cells of other origin (human or mice). Hingorani *et al.* generated a mouse model with conditional expression of endogenous LSL-$Kras^{G12D}$ allele to pancreatic progenitor cells, P48-Cre and Pdx1 that recapitulates the full spectrum of human pancreatic carcinogenesis with its precursor lesions and progress to PDAC (Hingorani *et al.* 2003). p48 is a transcription factor that is important for pancreatic development and is expressed early in pancreatic progenitor cells with relatively restricted expression in non-pancreatic cells. p48 is already in all pancreatic cells in early stages of organogenesis, but in mature cells it is restricted to acinar cells (Kawaguchi *et al.* 2002). The *LSL-KRAS^{G12D}* mouse strain harbours a mutant *KRAS* allele, that contains a glycine to aspartic acid transition in codon 12 with an upstream *STOP* cassette flanked by *LoxP* sites to prevent expression of this allele (Jackson *et al.* 2001). By crossing these mice with mice, harbouring tissue-specific Cre-recombinase (Pdx-1 or p48), the stop allele is excised and a pancreatic specific oncogenic KRAS expressing mouse model is generated (Hingorani *et al.* 2003). This oncogenic KRAS mutation leads to intrinsic and extrinsic GTPase activity with constitutive downstream signalling of Ras effector pathways (Hingorani 2003). These mice developed pancreatic cancer, resembling the human pancreatic cancer histologically as well as mimicking the development from normal acini to carcinoma-in-situ (Hingorani 2003). All three PanIN lesion stages were seen in those pancreata, similar to human PDAC only in small, intralobular ducts with mucus-producing goblet cells (Hingorani *et al.* 2003). Also similar to human PDAC,

it is the desmoplastic reaction with abundant stromal tissue observed in those mice strains (Hingorani *et al.* 2003). Based on this *KRAS* model, there have been created many further mouse models that contain various mutations, additionally to *KRAS*.

1.7 Aim of the study

Previous studies suggested that *PKD1* impairs the motility and invasiveness of tumor cells including pancreatic cancer cells. They also show a correlation between invasive tumor stages and low *PKD1* expression levels (Peterburs *et al.* 2009; Eiseler *et al.*, 2007, 2009, 2010; Wille *et al.* 2014). This data also indicates also a role for *PKD1* in pancreatic cancer and leads to the idea of a potential therapeutic target for PDAC.

The objective of my thesis is to characterize the effect of *PKD1* targeting in an oncogenic $KRAS^{G12D}$ mouse model. As a slow progressing mouse model, it is suitable to study pancreatic cancer development from early stages to fully developed tumor.

Aim 1: Characterisation of progression from ADM to PanINs

- The effect of *PKD1* knockout will be investigated by comparing the pancreata of 3 different mouse lines *(p48-Cre-$KRAS^{G12D}$; p48-Cre-$PKD1^{-/-}$; p48-Cre-$KRAS^{G12D}$-$PKD1^{-/-}$)* at 3 different time points (after 2, 5, and 9 months).
- The pancreas sections will be analysed for precursor lesions and other structural changes by immunohistochemical methods.

Aim 2: Characterisation of desmoplastic reaction

- We will analyse the composition of stroma to the outcome of *PKD1* targeting on tumorigenic microenvironment by immunohistochemical methods.

2. Material and Methods

2.1 Material

All the chemicals used in this study were purchased from Abcam (Cambridge, UK), AppliChem (Darmstadt, D), BD Phamingen (New Jersey, USA), MP Biomedicals, Cell Signalling (Frankfurt am Main, D), Carl Roth (Karlsruhe, D), Dako (Hamburg, D), Otto Fischar GmbH (Saarbrücken, D), Jackson Immunoresearch (Newmarket ,UK), Merck (Darmstadt, D), Monosan (Beutelsbach, D), Roche Diagnostics GmbH (Mannheim, D), Santa Cruz (Santa Cruz, USA), AbD Serotec (Puchheim, D), Serva Electrophoresis GmbH (Heidelberg, D), Sigma Aldrich (Munich, D), Thermo Scintific (Schwerte, D), Uniklinikum Apotheke Ulm (Ulm, D), Vector Lab (Loerrach, D) unless otherwise specified.

2.1.1 Buffers and Solutions

Following buffers and solutions were used:

2.1.1.1 PBS 1%, pH 7.4

Following ingredient were dissolved in 500 ml dH_2O:

Table 1: Ingredient dissolved in 500 ml distilled water for PBS 1% (Phosphate-buffered saline)

Substance	*Amount*
NaCl	4 g
KCl	0.1g
Na2HPO4	0.72 g
KH2PO4	0.12 g

2.1.1.2 Tris-Buffered Saline 0.05% TWEEN (TBS-T), pH7.6

Table 2: Ingredient dissolved in 500 ml distilled water for 0.05% TBS-T (Tris-buffered saline TWEEN)

Substance	*Amount*	*Company*
Tris Base	1.21 g	
NaCl	4 g	
TWEEN® 20	0.25 ml	Sigma Aldrich,#P7949

2.1.1.3 Eosin staining substance 0.1%

Table 3: Ingredient for Eosin staining dissolved in double-distilled water (ddH_2O)

Substance	*Amount*	*Company*
Eosin	0.1 g	Carl Roth GmbH, #70891
ddH2O	20 ml	
95% EtOH	80 ml	
70% EtOH	150 ml	
Acetic Acid	1 ml	

2.1.1.4 Alcian Blue Solution 1%, pH 2.5

1 g of Alcian Blue was dissolved in 100 ml of 3% acetic acid solution

2.1.1.5 Azokarmin G 1% solution

1 g Azokarmin G was dissolved in 1000 ml dH_2O, boiled and filtered. Then 10 ml Acetic acid was added and mixed again.

2.1.1.6 Aniline Blue 0.5% - Orange G 2% solution

5 g of Aniline Blue, 20 g of Orange G were dissolved in 1000 ml dH2O, boiled and filtered. Then 10 ml Acetic acid was added and mixed again.

2.2 Methods

We used following mouse lines:

1. PDAC promoting endogenous *KRAS*^{G12D} expressing mouse models under control of p48 promoter (*p48-Cre-KRAS*^{G12D}),
2. conditional pancreas specific *PKD1* knockout mouse model (*p48-Cre-PKD1*$^{-/-}$) and
3. a mouse model expressing oncogenic activated *KRAS* mutation and simultaneous knockout of *PKD1* under control of p48 promoter. (*p48-Cre-KRAS*^{G12D}*-PKD1*$^{-/-}$).

The animals were sacrificed after 2, 5 and 9months and the organs were collected for IHC stainings and protein analyses. These experiments were performed under approved conditions of the University Animal Care Committee and the Federal Authorities for animal research with the project license TVA1280 (Tübingen, Germany, according to "Tierschutzgesetz §8 Absatz1").

2.2.1 Tissue processing for immunohistochemistry

The tissues were fixed with 4% formaldehyde (Sigma-Aldrich), a semi-reversible, covalent crosslinking reagent. After fixing, the sections were processed in graded alcohol (70 %, 96 %, 100 % ethanol), Xylol and embedded in paraffin wax to maintain the original architecture. Cooled Tissue Paraffin blocks were cut in 5 µm thick sections, using the microtom (Thermo Scientific® Micron, HM355S). Then the sections were collected and positioned on a microscope slide (Roth LH25.1, #31023052), and dried overnight in a 58°C preheated incubator. In this state, the sections were stored until they were used for stainings.

2.2.2 Stainings

2.2.2.1 Hematoxylin, Eosin and Alcian blue stainings

Hematoxylin and eosin stain (H&E) is a widely used histological staining method to reveal tissue structures. It serves as a method to distinguish different morphological structures of an organ based on two different dyes. It is used to get a first overview of tissue formations for

further investigations and particular aspects. While Haemalaun stains basophil structures blue, eosin stains the eosinophil structures red. The following procedure was used:

For H&E staining, unstained sections were deparaffinized in graded alcohol and xylene and placed in Haemalaun for 1 min. The sections were thrn rinsed with water and placed in Eosin for 2 min. After rinsed again with water, the sections were dehydrated by graded alcohol series and xylene.

For Azan staining, after deparaffinization, the sections were placed in 58°C preheated Azokarmin for 15 min, 4 min in 1% Aniline, 1 min in Acetic acid alcohol, 30 min in 5% Phosphotungstic acid and 15 min in Aniline Blue-Orange G.

Alcian Blue staining was performed with Alcian Blue solution for 15 min after deparaffinization. After 2 min of rinsing with water, the sections were placed in Nuclear Fast Red for 5 min and afterwards dehydrated.

2.2.2.2 Immunohistochemistry

The Immunohistochemistry refers to a process used in medical and biological researches to detect proteins or other structures by using special antibodies for various antigen. This method is composed of three crucial sub-processes. These are: preparation of tissue, incubation with antibodies and the visualization of the antibody-antigen complex.

After deparaffinization and rehydration, the crosslinking of proteins which emerge during formalin fixation of the organ, the epitopes had to be revealed. To undo the crosslink, a heat-induced epitope retrieval (HIER) was used. As an alternative way to HIER, there was also used Proteinase for epitope retrieval in some stainings. Minimizing of non-specific staining requires therefore various blocking steps. The sections were blocked with 3% of hydrogen peroxide to clear the endogenous peroxidase activity, the Avidin-Biotin Blocking Kit (Vector Lab, #SP2001) to block the endogenous biotin and for each antibody a specific blocking serum (for more details see table 1).

To label and visualize the specific antigens an indirect staining method with an unlabelled primary antibody and a biotin labelled antibody was used. The biotin-labelled antibody was visualized the ABC-Kit was applied. This third layer with a peroxidase end can be detected with the NovaRED Kit (VectorLab, #SK-4800). This step is followed by a counter staining step with Mayers Haemalaun (Merck, #1.09249.2500).

Table 4: Additional specified information to the general IHC protocol described above

AB: *Antibody;* ***AUS:*** *Antigen Unmasking Solution (VectorLab, #H-3300);* ***DTRS:*** *Dako Target Retrieval Solution;* ***TRIS:*** *Tris(hydroxymethyl)aminomethane;* ***EDTA:*** *Ethylenediamine tetraacetic acid*

Epitop AB	*Retrieval Solution*	*AB Dilution*	*Secondary AB*
B220	AUS	1/200	Anti-Mouse
CD3	AUS	1/200	Anti-Rabbit
CD4	Tris-EDTA	1/50	Anti-Mouse
CD40	EDTA	1/50	Anti-Rat
CD45	DTRS	1/50	Anti-Rat
CD8	AUS	1/200	Anti-Mouse
CK19	AUS	1/200	Anti-Rat
COX2	AUS	1/300	Anti-Rabbit
F4/80	Proteinase K	1/800	Anti-Rat
LY6G	AUS	1/300	Anti-Rat

2.2.2.3 Imaging

The Keyence BZ-9000E (Biorevo) microscope was used to image the stained sections. The complete sections were imaged with 2x magnification to get an overview and the complete tissue size was calculated for normalization. The images were made with a 20x magnification to count stained cells. Analysis of IHC images were performed by imagej software (http://imagej.nih.gov/ij/)J. Cell counter plugin was used to count cells of complete tissue sections and colour deconvolution plugin was used to obtain percentage of the stained area. To compare different sections with various sizes, the number of cells were normalized to section size.

3. Results

3.1 Generating the P48-Cre-KRAS^{G12D}-PKD1$^{-/-}$ Mouse Model

To examine the role of PKD1 in pancreatic carcinogenesis we generated mouse model with pancreas specific *PKD1* knockout and concomitant expression of oncogenic *KRAS* under control of p48 promoter. Mouse model with oncogenic *KRAS* mutation are known for developing pancreatic cancer (Hingorani *et al.* 2003). The pancreas tissue specific *PKD1* knockout mouse line (*P48-Cre-PKD1*$^{-/-}$ mice) is generated by crossing of *PKD1*$^{loxP/loxP}$ mice (Fielitz *et al.* 2008) with *P48-Cre* mice (Dr. Armacki) (Figure 3).

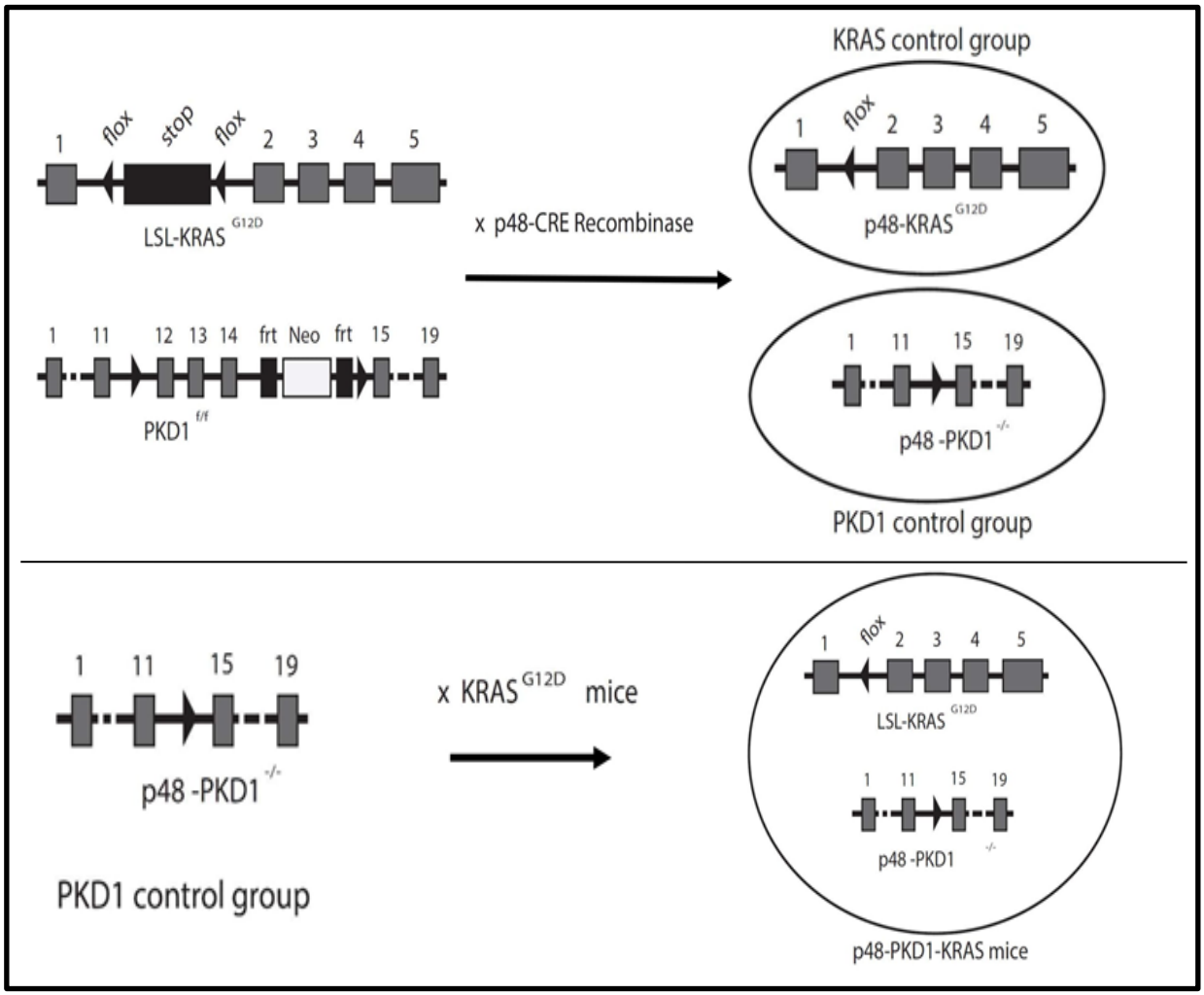

Figure 3: Schematic representation of generation of the mouse model with pancreas specific knockout and concomitant expression of oncogenic *Kras*

Conditional LSL-KRAS^{G12D} mice were crossed with mice that express Cre-recombinase from the pancreas specific promotor (p48) mice to obtain pancreas specific oncogenic KRAS^{G12D} mice. Pancreatic specific PKD1 knockout mice (p48-Cre-PKD1$^{-/-}$) were created using the same Cre-recombinase system. The Cre-recombinase system is used to carry out deletions at specific sites in the DNA of cells. To obtain p48-Cre-KRAS^{G12D}-PKD1$^{-/-}$ mice with concomitant expression of oncogenic

KRAS and PKD1 knockout, we crossed LSL-p48-KRAS^{G12D} mice with p48-PKD1$^{-/-}$ mice using also the Cre-recombinase system.

KRAS: *p48-Cre-KRAS^{G12D};* ***PKD1:*** *p48-Cre-PKD1$^{-/-}$;* ***KRAS-PKD1:*** *p48-Cre-KRAS^{G12D}-PKD1$^{-/-}$;* ***flox:*** *flanked by lox;* ***LSL:*** *lox-STOP-lox allele*

3.2 Pancreas specific knockout of PKD1 decreases survival

To evaluate the effect of *PKD1* knockdown in pancreatic cancer, we assessed mice over a period of 1 year. As expected, *p48-Cre-KRAS^{G12D}-PKD1$^{-/-}$* mice have a significantly shortened median survival of approximately 300 days as compared with their control littermate *p48-Cre-KRAS^{G12D}* (Figure 4).

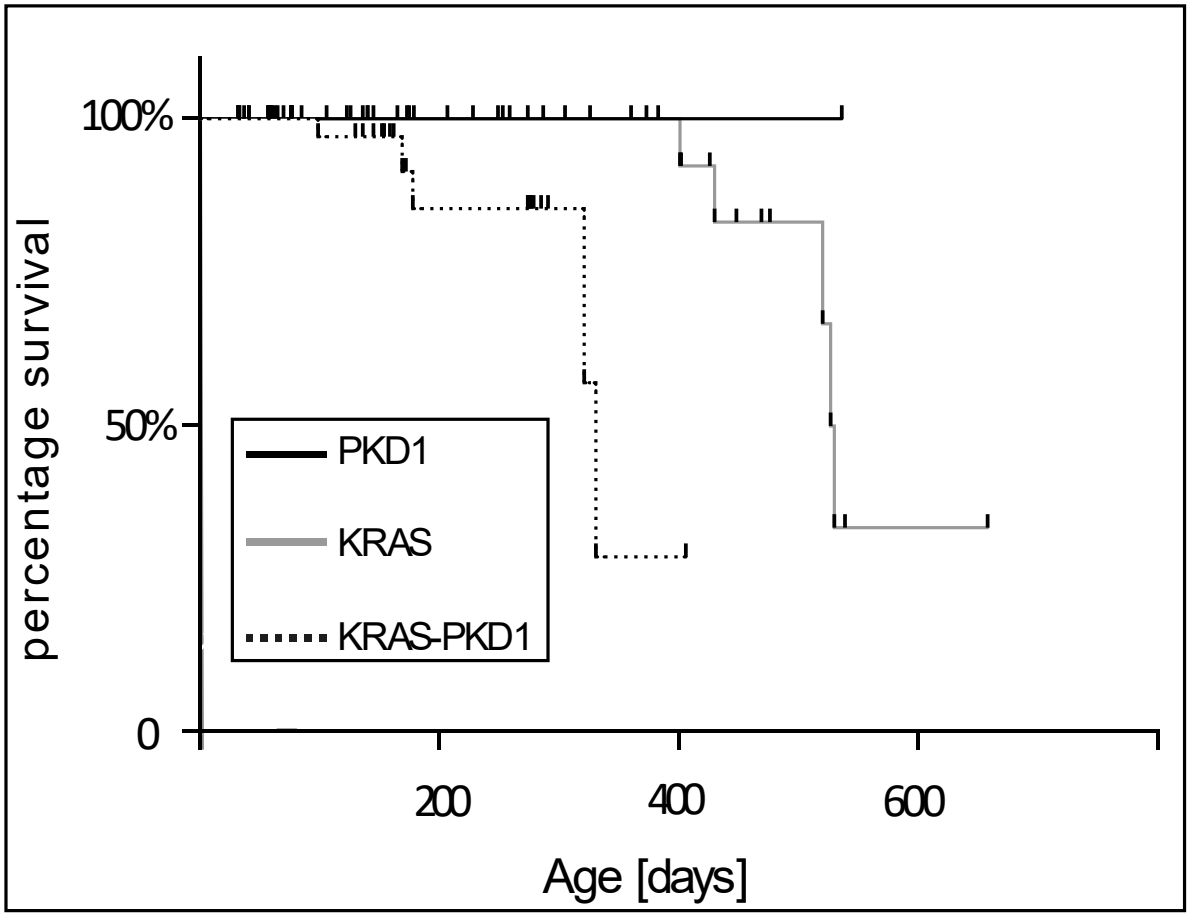

Figure 4: Survival of *p48-Cre-KRAS^{G12D}-PKD1$^{-/-}$* mice is significantly decreased
Kaplan-Meier curves reveal the median survival of all three mice groups. p48-Cre-KRAS^{G12D}-PKD1$^{-/-}$ mice have an approximately 200 days less median survival rate than p48-Cre-KRAS^{G12D} mice. In p48-Cre-KRAS^{G12D}-PKD1$^{-/-}$ mice, 100% mortality occurred by about 400 days, whereas the last p48-Cre-KRAS^{G12D} mice lived about 650 days.
KRAS: *p48-Cre-KRAS^{G12D};* ***PKD1:*** *p48-Cre-PKD1$^{-/-}$;* ***KRAS-PKD1:*** *p48-Cre-KRAS^{G12D}-PKD1$^{-/-}$*

p48-Cre-KRAS^{G12D}-PKD1$^{-/-}$ mice (n=18), 100% mortality occurred after 400 days whereas the last *p48-Cre-KRAS^{G12D}* (n=20) mice died after approximately 700 days (Figure 4). Median survival of *p48-Cre-KRAS^{G12D}-PKD1$^{-/-}$* mice was 331 days, whereas *p48-Cre-KRAS^{G12D}* mice had a median survival of 527 days. This is correlating with PDAC development:

Table 2: *p48-Cre-KRAS^{G12D}-PKD1$^{-/-}$* mice already develop PDAC at age of 5 months

Table shows mouse strains and percentage of mice which have developed PDAC at several time points.

PDAC: *Pancreatic ductal adenocarcinoma*

Mouse Strain	*p48-Cre-PKD1$^{-/-}$*			*p48-Cre-KRAS^{G12D}*			*p48-Cre-KRAS^{G12D}-PKD1$^{-/-}$*		
Age [months]	2	5	9	2	5	9	2	5	9
% PDAC	0%	0%	0%	0%	0%	50%	0%	58%	70%

3.3 Histo-pathological examination revealed a significant Tumor progression in *P48-Cre-KRAS^{G12D}-PKD1$^{-/-}$* mice

The H&E staining in 2-months-old *p48-Cre-KRAS^{G12D}-PKD1$^{-/-}$* mice show already beginning structural changes like ductal changes (ADMs) and stromal deposit, whereas in *p48-Cre-KRAS^{G12D}* and *p48-Cre-PKD1$^{-/-}$* mice we mostly see normal/healthy tissue (Figure 5). A significant disease burden did become apparent in *p48-Cre-KRAS^{G12D}-PKD1$^{-/-}$* mice at the age of 5 months. Early stage PanIN lesions were rarely seen in 5-months-old *p48-Cre-KRAS^{G12D}* mice. They showed small areas of stromal tissue and PanINs in low stages, whereas *p48-Cre-KRAS^{G12D}-PKD1$^{-/-}$* mice progressed further in tissue impairment, in terms of more desmoplastic areas and PanIN lesions. 9-months-old *p48-Cre-KRAS^{G12D}-PKD1$^{-/-}$* mice showed the full spectrum of preinvasive lesions with PDAC development in almost all mice of this group. On the contrary, *PKD1* control mice didn't show any pathological changes at any time point, not even after 9 months.

To identify the characteristics of PanIN, immunohistochemistry against CK19 and Alcian blue staining were performed (Figure 6). A feature of PanIN lesions is the abundant mucin content which was demonstrated by Alcian Blue staining (Figure 6A). The epithelial nature of PanIN lesions and visualizing the acinar cells which presented with acinar-to-ductal metaplasia (ADM) process we performed a CK-19 staining, an epithelial marker for duct-like cells in pancreas tissue sections (Figure 6B).

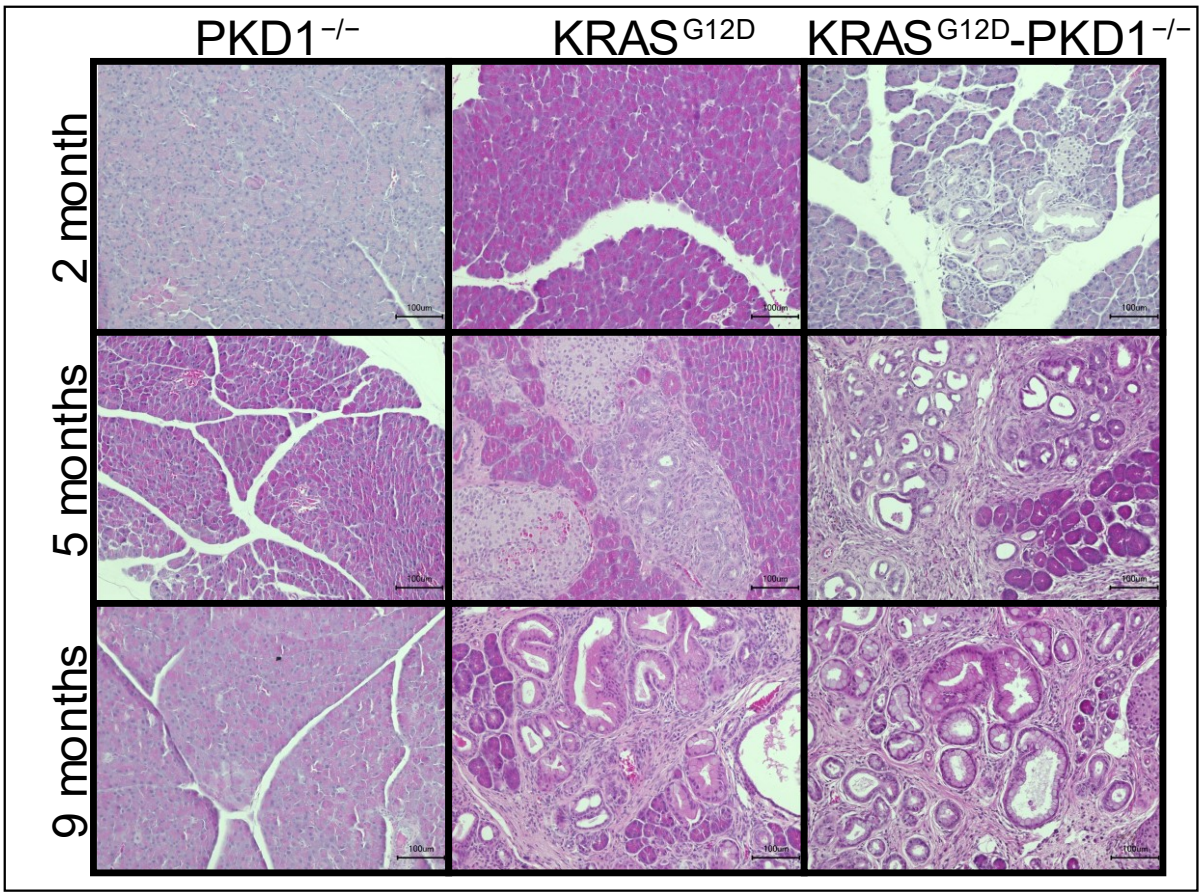

Figure 5: Hematoxylin and eosin (H&E) staining for general impression of Pancreatic ductal adenocarcinoma development

Graph shows representative images of H&E staining. It shows an unspecific change in tissue architecture in already 5-months-old p48-Cre-KRAS^{G12D}-PKD1$^{-/-}$ mice. Almost no healthy acinar structures are seen in 9-months-old p48-Cre-KRAS^{G12D} and p48-Cre-KRAS^{G12D}-PKD1$^{-/-}$ which have developed pancreatic cancer. Size bars indicate 100 µm.

KRAS^{G12D}: *p48-Cre-KRAS^{G12D};* ***PKD1$^{-/-}$:*** *p48-Cre-PKD1$^{-/-}$;* ***KRAS^{G12D}-PKD1$^{-/-}$:*** *p48-Cre-KRAS^{G12D}-PKD1$^{-/-}$*

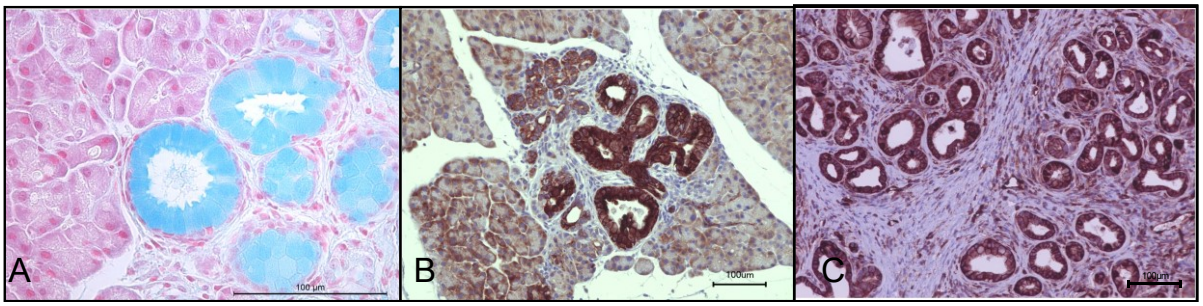

Figure 6: Characterization of Pancreatic intraepithelial neoplasia (PanIN) lesions

Alcian blue stain shows abundant mucin content (A) in PanINs that have undergone an acinar-to-ductal transdifferentiation and Cytokeratin-19 (CK19) shows the epithelial nature of these lesions (B). Cyclooxygenase 2 (COX2) activation is seen in almost all PanINs, that indicates a permanent inflammatory reaction in these lesions (C). Size bars indicate 100 µm.

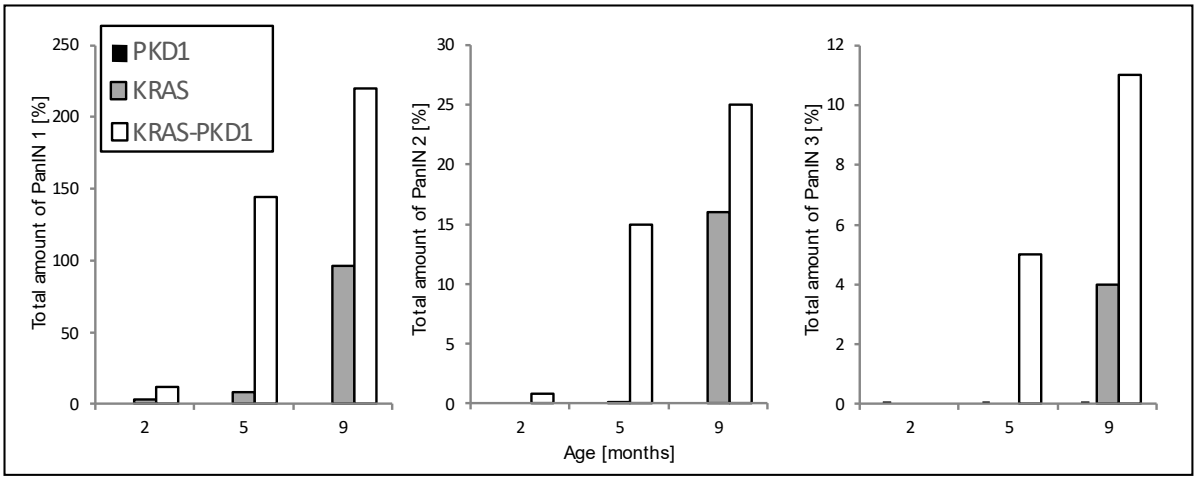

Figure 7: Histologic progression of Pancreatic intraepithelial neoplasia (PanIN) lesions over time

Graph shows distribution of PanINs in percentages (+/- SEM) of all neoplastic ducts. They were separated by PanIN grade (PanIN-1, -2 and -3) in 3 different mouse lines of average age 2, 5 and 9 months. p48-Cre-KRAS^{G12D}-PKD1$^{-/-}$ mice contain already in 5-months-old animals abundant PanIN lesions. Comparable amounts of precursor lesions were seen in 9-months-old animals of p48-Cre-KRAS^{G12D} animals. PanINs were count per pancreas section and ratio to section size was calculated.
KRAS: *p48-Cre-KRAS^{G12D};* ***PKD1:*** *p48-Cre-PKD1$^{-/-}$;* ***KRAS-PKD1:*** *p48-Cre-KRAS^{G12D}-PKD1$^{-/-}$*
SEM: *Standard error of the mean*

Pancreata of 2-months-old *p48-Cre-KRAS^{G12D}-PKD1$^{-/-}$* mice show abundance of ADMs and type I PanINs. The number and grade of PanIN lesions increase with age. *p48-Cre-KRAS^{G12D}-PKD1$^{-/-}$* mice ultimately develop invasive PDAC at age of 5 months with following increase in tumor incidence as mice age to 9 months (Figure 7). Whereas the vast majority of the pancreatic parenchyma of 2- and 5-months-old *p48-Cre-KRAS^{G12D}* mice were histologically normal with scattered PanIN I lesions, a significant disease burden did become apparent in 9-months-old *p48-Cre-KRAS^{G12D}* animals with an increase of PanIN I, II and III lesions (Figure 7). These data suggest that loss of *PKD1* facilitates oncogenic *KRAS* triggered development of pancreatic cancerogenesis.

3.4 Progression of the precancerous lesions to pancreatic cancer is accompanied by development of rich desmoplastic reaction in p48-Cre-KRAS^{G12D}-PKD1$^{-/-}$mice

Progression of the precancerous lesion to pancreatic cancer in *p48-Cre-KRAS^{G12D}-PKD1$^{-/-}$* mice was accompanied by rich desmoplastic reaction, manifested by inflammatory cell infiltrations and extracellular matrix deposits. 2-month-old *p48-Cre-KRAS^{G12D}-PKD1$^{-/-}$* mice showed scattered foci of stroma surrounding early precancerous lesions. In pancreata of 5-months-old *p48-Cre-KRAS^{G12D}-PKD1$^{-/-}$* mice, the vast majority of parenchyma was replaced by desmoplastic reaction comprised of inflammatory cells, fibroblasts, and collagen deposition. A similar extend of stromal tissue was seen in 9-months-old *p48-Cre-KRAS^{G12D}* mice (Figure 8).

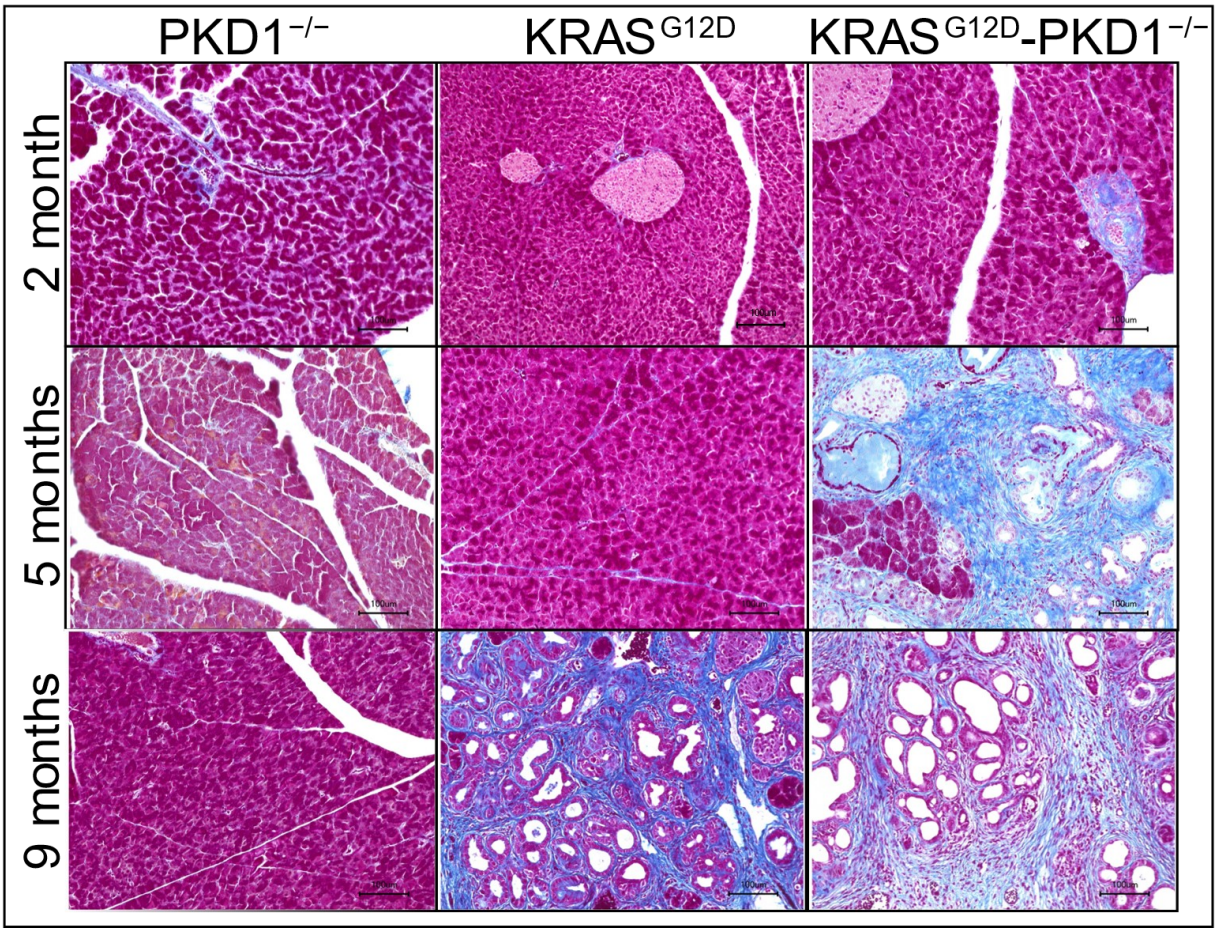

Figure 8: Increasing desmoplasia visualized by Azan staining

Graph shows representative images of collagen deposit in pancreatic tissue, especially in cancer tissue. Increasing desmoplastic reaction is shown by Azan staining in already 5-months-old p48-Cre-KRAS^{G12D}-PKD1$^{-/-}$ mice. Desmoplastic areas contain collagen deposits which are showed as blue areas. The graph shows representative pancreatic tissues of 9-months-old p48-Cre-KRAS^{G12D}-PKD1$^{-/-}$ and p48-Cre-KRAS^{G12D} mouse pancreata with an almost completely replaced tissue with desmoplasia. Size bars indicate 100 µm.

KRAS^{G12D}: *p48-Cre-KRAS^{G12D};* ***PKD1$^{-/-}$:*** *p48-Cre-PKD1$^{-/-}$;* ***KRAS^{G12D}-PKD1$^{-/-}$:*** *p48-Cre-KRAS^{G12D}-PKD1$^{-/-}$*

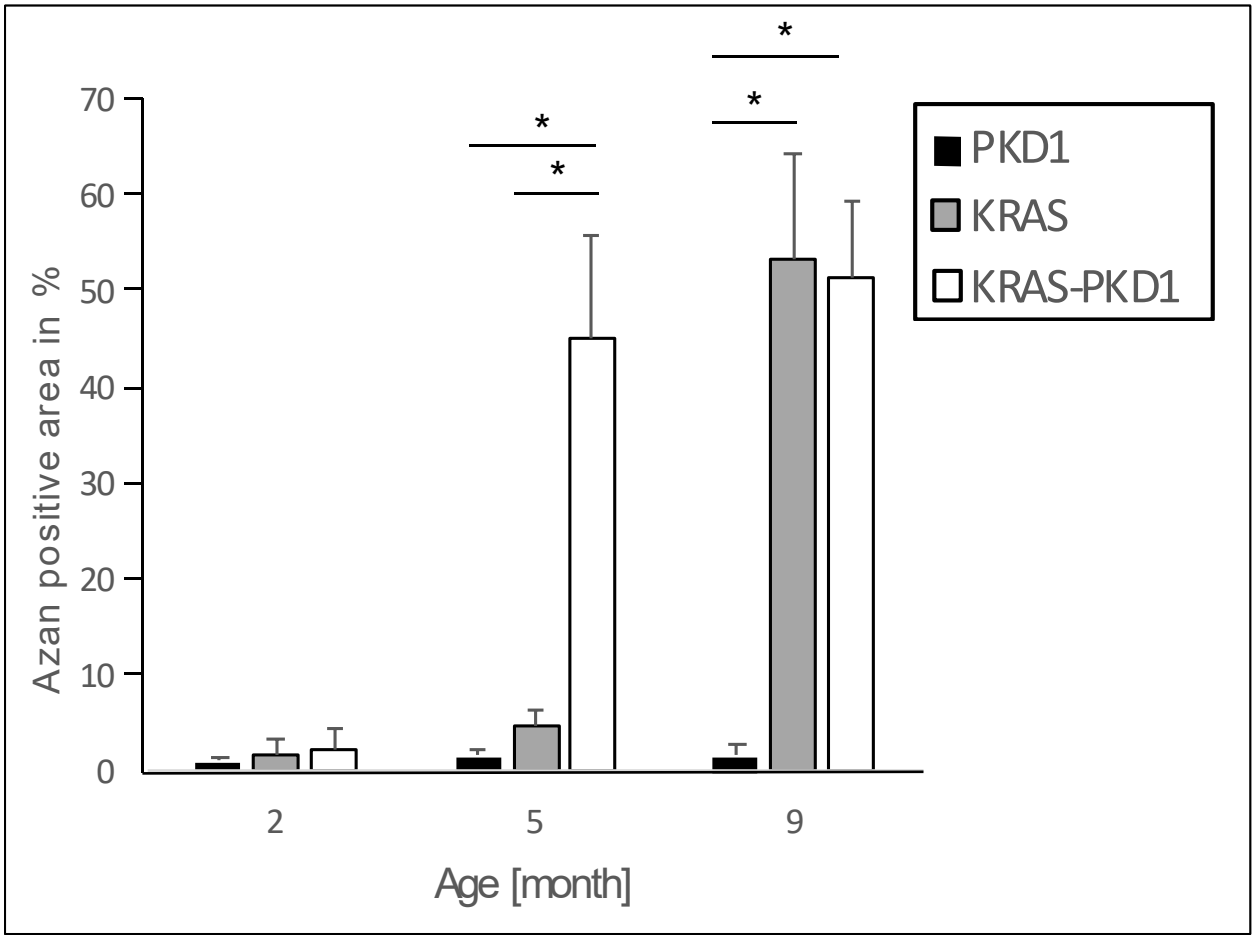

Figure 9: Severe desmoplastic areas are seen in already 5-months-old *p48-Cre-KRAS^{G12D}-PKD1$^{-/-}$* mice

Graph shows percentage of collagen deposit in pancreatic tissue that was marked by Azan staining. The areas were measured, and the percentage of stained area was calculated relative to the whole section size. We can see that almost half of the complete pancreatic tissue is replaced by collagen in 5-and 9-months-old p48-Cre-KRAS^{G12D}-PKD1$^{-/-}$ as well as in p48-Cre-KRAS^{G12D} mice. Statistically significant differences between groups are marked by an asterisk. Bars represent mean values ± SEM of three different mouse lines and age groups; ∗P < 0.05.

KRAS: *p48-Cre-KRAS^{G12D};* ***PKD1:*** *p48-Cre-PKD1$^{-/-}$;* ***KRAS -PKD1:*** *p48-Cre-KRAS^{G12D}-PKD1$^{-/-}$*

The percentage of desmoplastic areas were measured and visualized in Figure 9. These results suggest a fibrogenesis preventing function of active *PKD1* in oncogenic *KRAS* mice. It seems that the desmoplastic reaction is rapidly increased by knockout of *PKD1* in pancreatic *KRAS* mouse models compared to mice with only oncogenic KRAS mutation (*p48-Cre-KRAS^{G12D}*). *PKD1* knockout mice (*p48-Cre-PKD1$^{-/-}$*) show no significant pancreatic lesions. This indicates that *PKD1* knockdown mice without any other oncogenic mutation have no pancreatic cancer initiation function. Next, we decided to continue with further experiments to explore the cell composition of stroma in our mouse models.

3.5 Increasing influx of leukocytes during PDAC progression

Another characteristic feature of PanINs and pancreatic cancer is activation of COX2. To determine how *PKD1* knockdown affects COX-2 in pancreatic cancer and its precursor lesions, we performed a COX-2 immunohistochemistry staining. We observed a significant difference in COX-2 expression between cancerous tissues and the non-cancerous tissues (Figure 9). There is also a significant difference between 5-months-old *p48-Cre-KRAS^{G12D}* and *p48-Cre-KRAS^{G12D}-PKD1$^{-/-}$*. 5-months-old *p48-Cre-KRAS^{G12D}-PKD1$^{-/-}$* mice have much higher COX-2 activation levels then the other mouse lines. These data correlate with PanIN and cancer levels in those mice. Strong reaction for COX-2 was observed in the cytoplasm of PanINs and scattered cells within stromal tissue, but not in normal pancreatic parenchyma (Figure 6C).

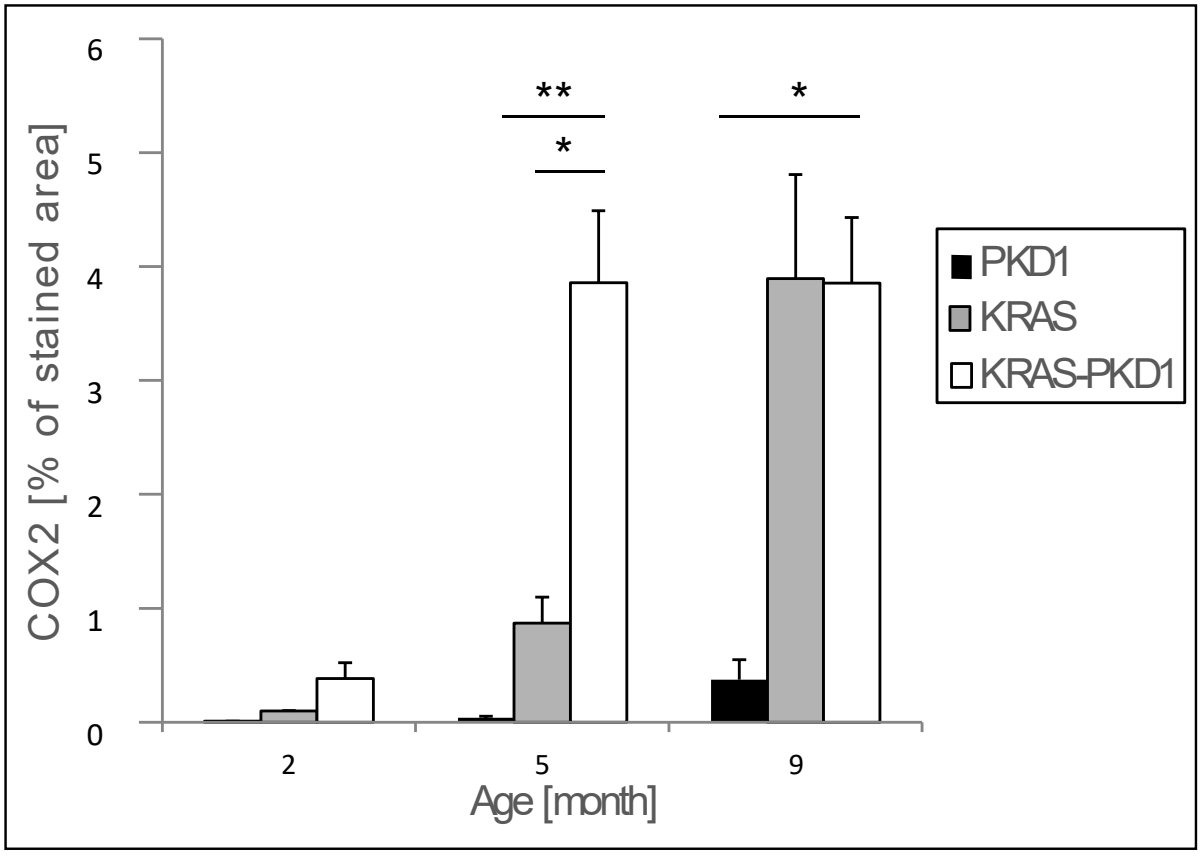

Figure 10: Measurements of Cyclooxygenase 2 (COX2) activation

The comparison of COX2 activity between the different mice groups. In 5-months-old p48-Cre-KRAS^{G12D}-PKD1$^{-/-}$ mice, a strong activation of COX2 is seen. Similar extend of COX2 activation was only seen in 9-months-old p48-Cre-KRAS^{G12D}. Bars represent mean values ± SEM of three different mouse lines and age groups; *P < 0.05 and **P < 0.01.

KRAS: *p48-Cre-KRAS^{G12D};* ***PKD1:*** *p48-Cre-PKD1$^{-/-}$;* ***KRAS -PKD1:*** *p48-Cre-KRAS^{G12D}-PKD1$^{-/-}$*

To determine the presence of leukocytes in desmoplastic areas, we characterized cells expressing the leukocyte common antigen (CD45) in pancreas by immunohistochemistry staining (Figure 11). The stained areas were measured by imagej and percentage of $CD45^+$ cell areas were calculated (Figure 12).

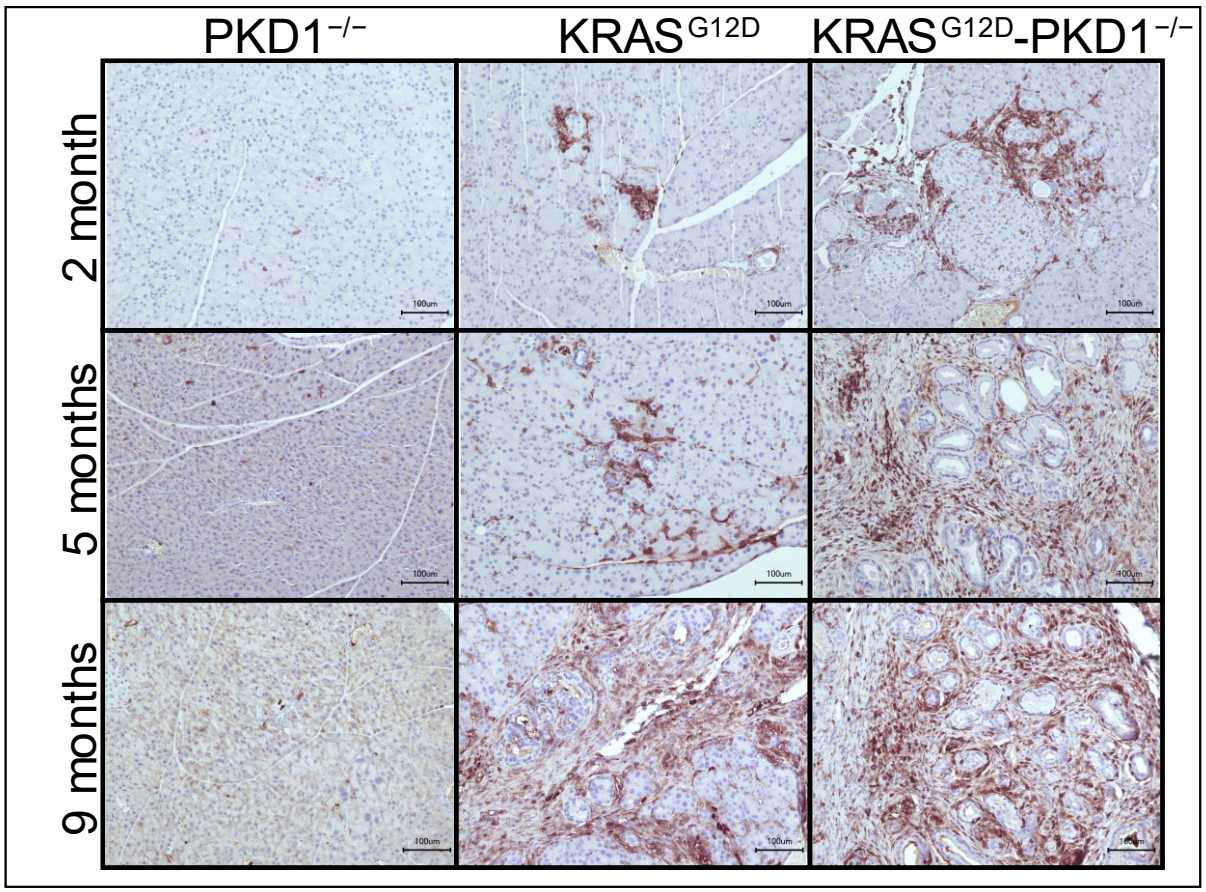

Figure 11: IHC staining for CD45 positive cells, CD45 is a leukocyte common antigen.
Representative pictures of CD45$^+$ cells (brown areas) in pancreas sections of three different mouse lines. We see a significant presence of leukocytes in 5-months-old p48-Cre-KRAS^{G12D}-PKD1$^{-/-}$, whereas p48-Cre-KRAS^{G12D} mice show a significant influx only in 9-months-old animals. p48-Cre-PKD1$^{-/-}$ mice do not show any influx of CD45$^+$ positive cells. An only PKD1 loss does not lead to pancreatic cancer development. Size bars indicate 100 µm.
KRAS^{G12D}: *p48-Cre-KRAS^{G12D};* ***PKD1$^{-/-}$:*** *p48-Cre-PKD1$^{-/-}$;* ***KRAS^{G12D}-PKD1$^{-/-}$:*** *p48-Cre-KRAS^{G12D}-PKD1$^{-/-}$*

We saw a progressive infiltration of $CD45^+$ cells from healthy tissue to preinvasive PanIN and invasive PDAC. The most and fastest influx was seen in *p48-Cre-KRAS^{G12D}-PKD1$^{-/-}$*mice. These mice display already after 2 months an influx of $CD45^+$ cells with rapid increase that is seen in 5- and 9-months-old mice (Figure 12). Pancreata of mice with histologically normal pancreatic tissue and mice with less PanINs contained only few $CD45^+$ cells except in *p48-Cre-KRAS^{G12D}-PKD1$^{-/-}$*mice. The tissues of 2-months-old *p48-Cre-KRAS^{G12D}-PKD1$^{-/-}$*mice were

mostly normal, but we still could see significant amounts of $CD45^+$ cells. These findings suggest a missing leucocyte suppressing function when *PKD1* is knocked down. An influx of relevant $CD45^+$ cells in *p48-Cre-KRAS^{G12D}* mice was seen in 5-months-old animals with an increase in the 9-months-old animals. No relevant cells were found in *p48-Cre-PKD1$^{-/-}$*mice (Figure 12). Increased stromal tissue and PanIN levels lead to concurrent increasing $CD45^+$ leukocytes clustered preferentially around PanINs and stromal areas. $CD45^+$ infiltration was even more intense in areas with dense fibrotic/carcinomatous tissue.

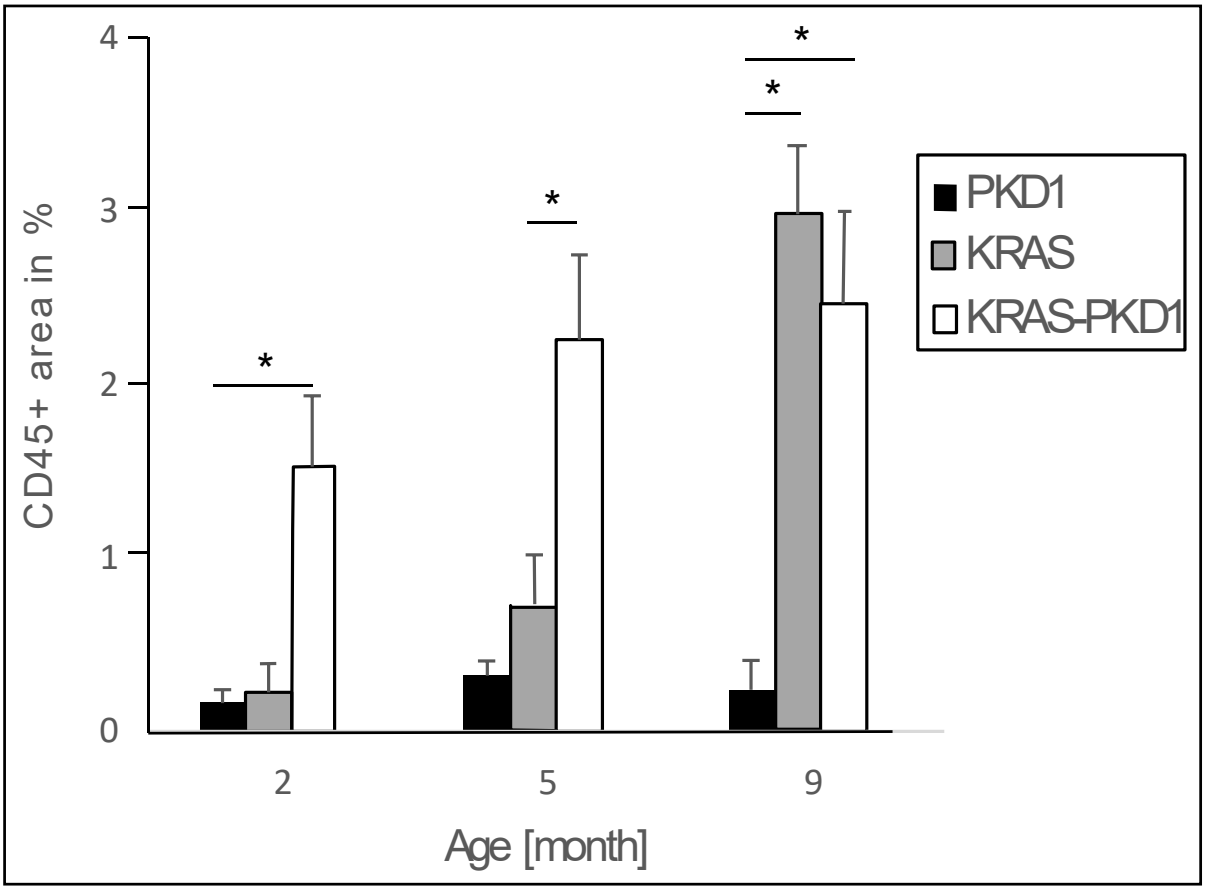

Figure 12: Measurements of $CD45^+$ areas in pancreas sections

Graph shows the percentage of $CD45^+$ cells influx in pancreatic tissue were measured and visualized. PKD1 knockout with oncogenic KRAS mutation lead to an early influx of leucocytes in 2-months-old animal that indicates a leucocyte preventing function for PKD1. The graph also shows a strong infiltration in pancreatic cancer in later stages. Bars represent mean values ± SEM of three different mouse lines and age groups; *P < 0.05.

KRAS: *p48-Cre-KRAS^{G12D};* ***PKD1:*** *p48-Cre-PKD1$^{-/-}$;* ***KRAS -PKD1:*** *p48-Cre-KRAS^{G12D}-PKD1$^{-/-}$*

For further characterization of $CD45^+$ cell composition, we performed immunohistochemistry stainings, directed against marker for the macrophages. Macrophages are reported to be present in early as well as later stages of PDAC, able to promote or suppress growth, depending on the predominant subgroup of macrophages (Clark *et al.* 2007). We could detect no significant

presence of macrophages in any of the three mouse strains in 2-months-old mice, using the murine macrophage marker F4/80 (Figure 13 and 14). We saw that disease progression to PDAC was accompanied by an increasing infiltration of F4/80^{+} macrophages (Figure 14). In 5 months *p48-Cre-KRAS^{G12D}-PKD1$^{-/-}$* mice, a rapidly increasing infiltration of macrophages was seen, which shows a COX-2 similar pattern. In 5-months-old *p48-Cre-KRAS^{G12D}* mice, there were only smaller amounts of detectable macrophages, significantly less than same-aged *p48-Cre-KRAS^{G12D}-PKD1$^{-/-}$*mice. Our findings show that an increased influx of macrophages is accompanied with increasing tumor/carcinoma development. This indicates a pro-tumorigenic function for macrophages in pancreatic cancer which is accelerated by *PKD1* knockout. After macrophages, we focused on T-lymphocytes which play an important role in pancreatic cancer and its microenvironment.

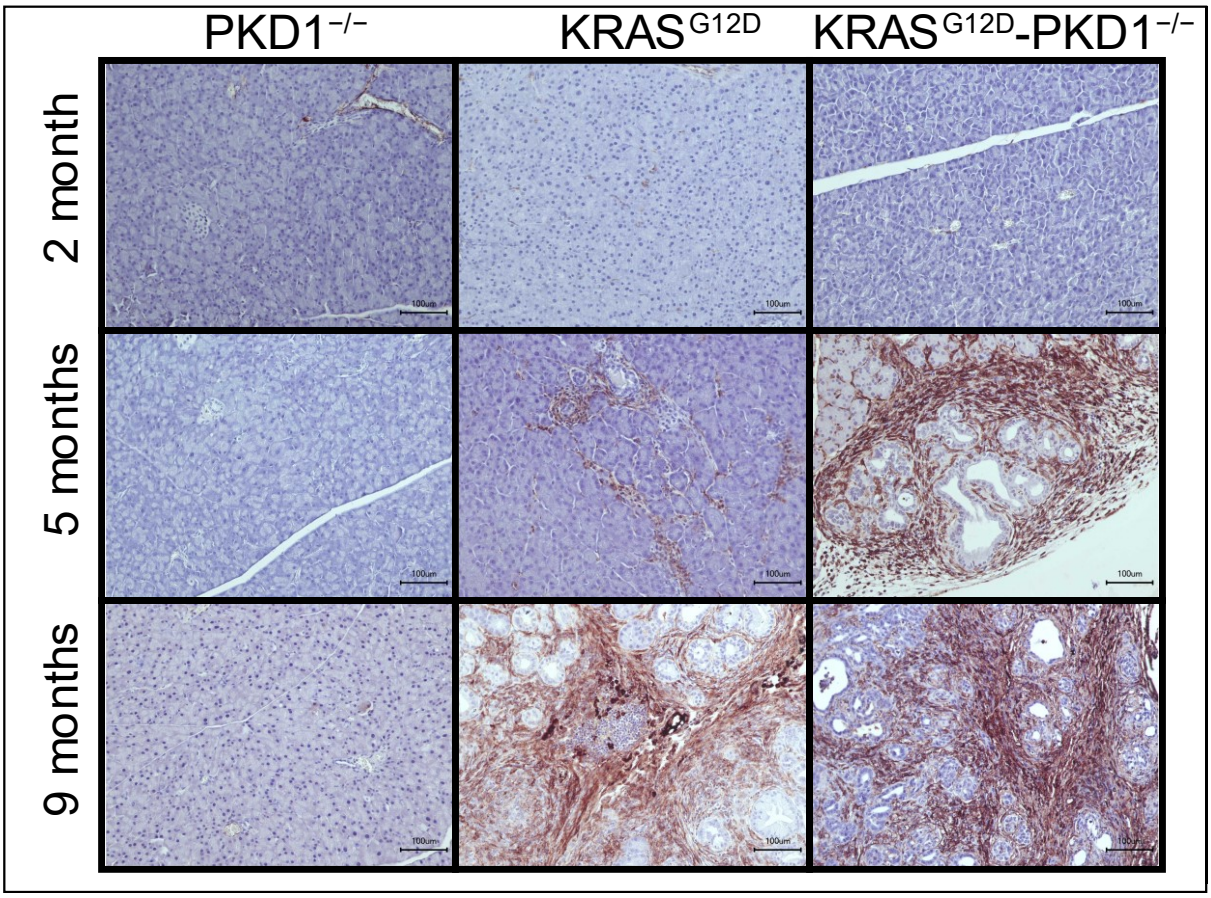

Figure 13: IHC staining for F4/80 positive cells (macrophages)

Graph shows representative images of the three different mouse lines with marked macrophages. F4/80+ marker is used to visualize macrophages (brown areas) by IHC staining. They were only seen in pancreata which already developed a pancreatic cancer. This development is similar to our results for Cyclooxygenase 2 (COX2) that indicates a positive correlation between these two cell types as well as a pro-tumorigenic function for macrophages. Size bars indicate 100 µm. KRAS^{G12D}: *p48-Cre-KRAS^{G12D};* ***PKD1$^{-/-}$:*** *p48-Cre-PKD1$^{-/-}$;* ***KRAS^{G12D}-PKD1$^{-/-}$:*** *p48-Cre-KRAS^{G12D}-PKD1$^{-/-}$*

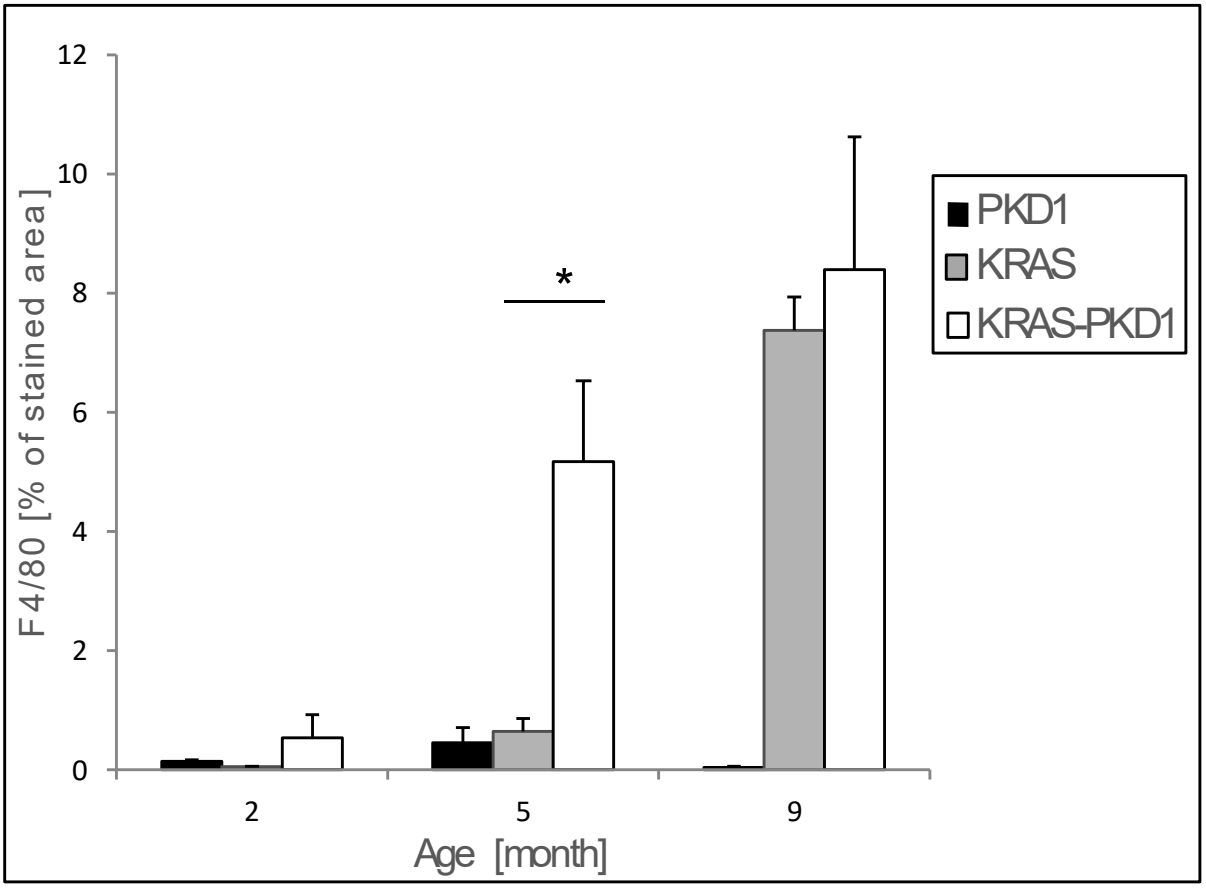

Figure 14: Infiltration of macrophages in pancreas sections

Graph shows the influx of macrophages in our three mouse models. Macrophages in pancreas sections were measured by imagej and calculated. Like leucocyte infiltration, there is seen a significant early influx of macrophages in 5-months-old p48-Cre-KRAS^{G12D}-PKD1$^{-/-}$ mice which have already developed cancer. A similar significant increase of macrophages in p48-Cre-KRAS^{G12D}mice is seen in 9-months-old animals. Bars represent mean values ± SEM of three different mouse lines and age groups; *P < 0.05.

KRAS: *p48-Cre-KRAS^{G12D};* ***PKD1:*** *p48-Cre-PKD1$^{-/-}$;* ***KRAS -PKD1:*** *p48-Cre-KRAS^{G12D}-PKD1$^{-/-}$*

CD3, a general marker for T-lymphocytes, was used to identify these cells in the pancreata of our mice (Figure 15). CD3^{+} T cells were seen rarely in normal pancreata, but in *p48-Cre-KRAS^{G12D}-PKD1$^{-/-}$* mice, we see an increasing CD3^{+} cell influx in already 2-month-old mice, a similar trend to CD45^{+} cells that suggests that most of those cells in healthy tissue are T-lymphocytes. Further progression of PanINs and PDAC is accompanied by a progressive infiltration of CD3^{+} T cells (Figure 16). These cells are found mostly in and around stromal tissue, rarely seen between and adjacent to PanIN lesions or cancer cells. There is seen a significant infiltration of CD3^{+} cells in 5-months-old *p48-Cre-KRAS^{G12D}* mice compared to mice with only *KRAS^{G12D}* mutation (Figure16). Further increase of CD3^{+} cells are seen in 9-

months-old animals with *KRAS^{G12D}* mutation, together with PDAC development (Figure 16). We never see any T-lymphocyte infiltration in *p48-Cre-PKD1$^{-/-}$* mice (Figure 16). The infiltrating T cells are divided in to CD4 and CD8 positive cells and were separately examined by immunohistochemistry stainings. Quantification of CD8$^+$ cells shows a significant increase in 9-months-old *p48-Cre-KRAS^{G12D}* and *p48-Cre-KRAS^{G12D}-PKD1$^{-/-}$* mice with PDAC development (Figure 17). But 5-months-old *p48-Cre-KRAS^{G12D}-PKD1$^{-/-}$* mice suggest an already early infiltration of CD8$^+$ cells (Figure 16). Clustered CD8$^+$ cells were often seen in stromal tissue, but rarely adjacent to PanIN areas. Like CD8$^+$ cells, CD4$^+$ lymphocytes are seen in fibrotic areas surrounding PanIN areas, but not often seen within PanIN areas (Figure 15). An infiltration of CD4$^+$ positive cells can be seen in earlier stages of disease (Figure 19). Already in 2-months-old *p48-Cre-KRAS^{G12D}* and *p48-Cre-KRAS^{G12D}-PKD1$^{-/-}$* mice we see infiltrating CD4$^+$ T-lymphocytes. The number of cells in those mice is increasing over time, hence we see in 9-months-old mice a further, strong increase of CD4 T-lymphocytes (Figure 19 and 20). T-lymphocytes in pancreata without PDAC development, do not show many infiltrating T-cells (Figure 18 and 20).

In conclusion, we see an increasing infiltration of CD4 and CD8 positive cells in pancreatic cancer, positively correlating with its progression. But we don't see many T-lymphocytes around PanIN areas or cancer cells. Most of those cells, especially CD8$^+$ cells, are within stromal tissue and do not reach to PanIN lesions. *PKD1* loss facilitates T-lymphocyte infiltration in mice with *KRAS^{G12D}* mutation which has already developed PDAC. Mice in early disease stages with only PanIN lesions show less infiltration ratio than in PDAC mice. T-cell-dependent antitumor immunity is thought to activated by CD40. Those cells are important in B- and T-cell proliferation and has therefore an immune regulatory function which is recently considered as a TAMs targeting pathway (Beatty *et al.* 2017). We detected them by immunohistochemistry staining and the infiltration was counted for each section. Our results show a beginning infiltration of CD40$^+$ cells in 5-months-old *p48-Cre-KRAS^{G12D}-PKD1$^{-/-}$* mice, whereas p48-Cre-KRAS^{G12D} do not show those cells in 5-months-old animal. A strong CD40$^+$ cell infiltration was seen in 9-months-old *p48-Cre-KRAS^{G12D}* and *p48-Cre-KRAS^{G12D}-PKD1$^{-/-}$* mice (Figure 21). The CD40$^+$ cells were rather associated in stromal sites than directly associated with PanIN lesions as seen.

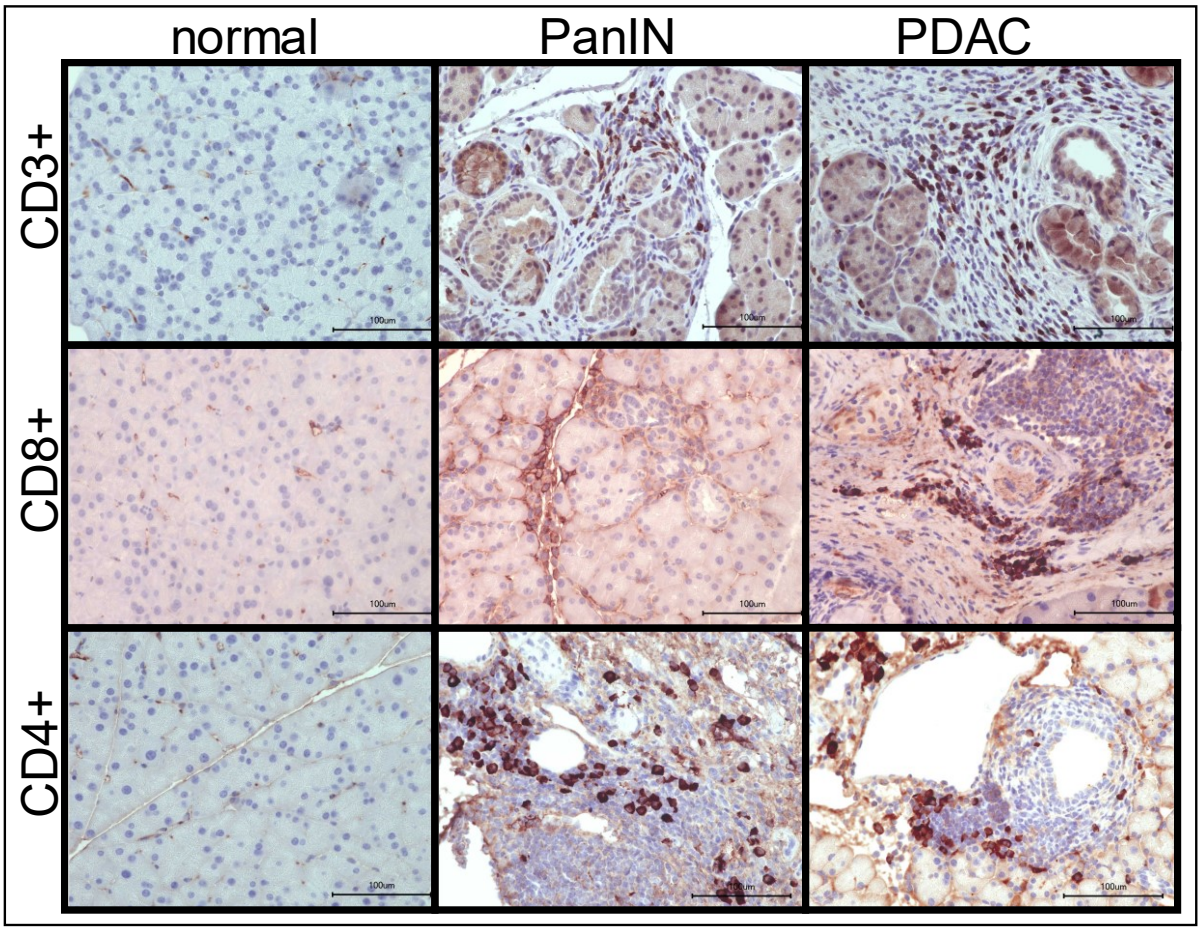

Figure 15: IHC staining for T-Lymphocytes

Representative pictures of T-lymphocytes in pancreas sections of three different tissue types (normal tissue, pancreata which had not developed carcinoma yet (PanIN) and pancreata with PDAC). CD3 marker is used to detect all T-cell subtypes. Additional, visualizations of subtypes are performed using CD4 and -8 markers. Size bars indicate 100 µm.

normal: *normal pancreatic tissue;* ***PanIN:*** *mouse that contain PanIN lesions but had not developed carcinoma yet;* ***PDAC:*** *mouse that have developed pancreatic ductal adenocarcinoma*

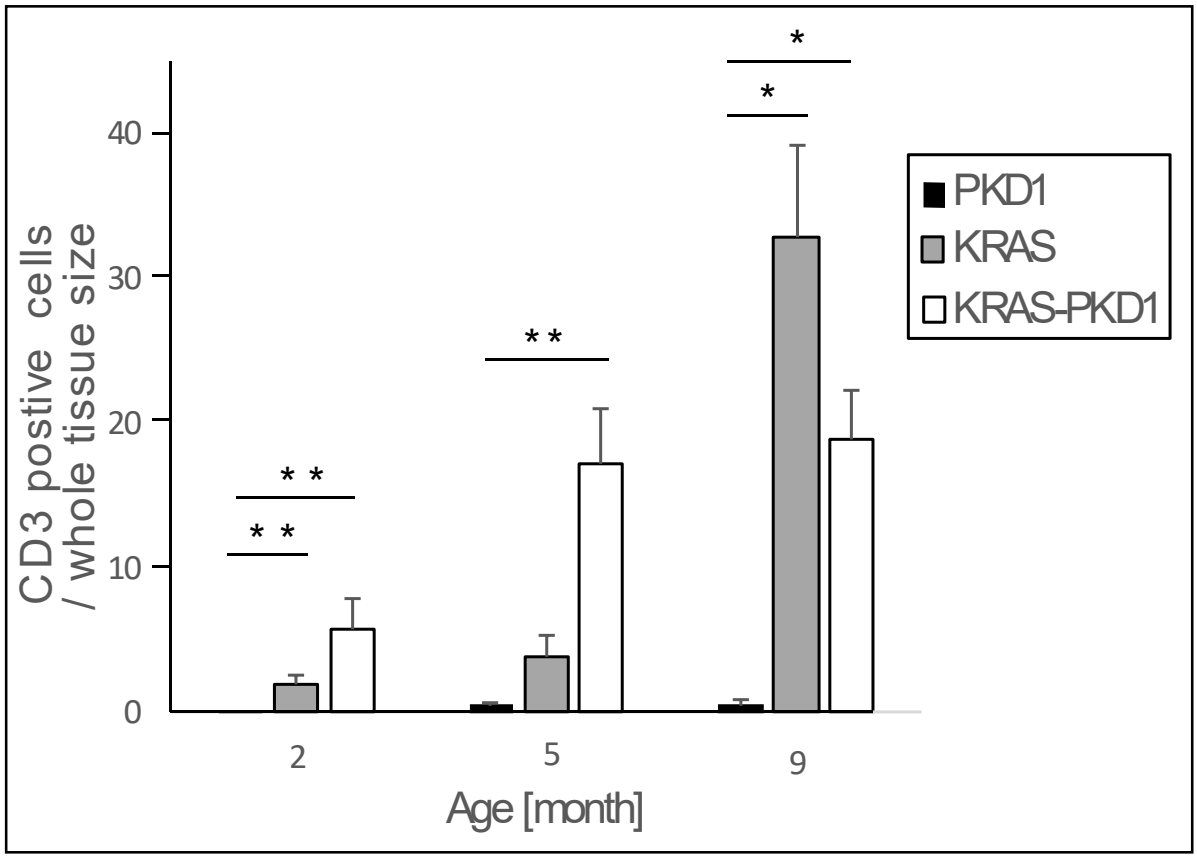

Figure 16: Quantification of infiltrating CD3$^+$ T-cells

CD3$^+$ stained cells were counted and ratio to tissue size was calculated. We see an early T-lymphocyte infiltration in already 2-months-old p48-Cre-KRAS^{G12D}-PKD1$^{-/-}$ and p48-Cre-KRAS^{G12D} mice. We see the infiltration in already normal pancreata which indicate an early effect of T-lymphocytes. A rapid increase in p48-Cre-KRAS^{G12D}mice are correlating with late PDAC development. Bars represent mean values ± SEM of three different mouse lines and age groups; ∗P < 0.05; ∗∗P < 0.01.
KRAS: *p48-Cre-KRAS^{G12D};* ***PKD1:*** *p48-Cre-PKD1$^{-/-}$;* ***KRAS -PKD1:*** *p48-Cre-KRAS^{G12D}-PKD1$^{-/-}$*

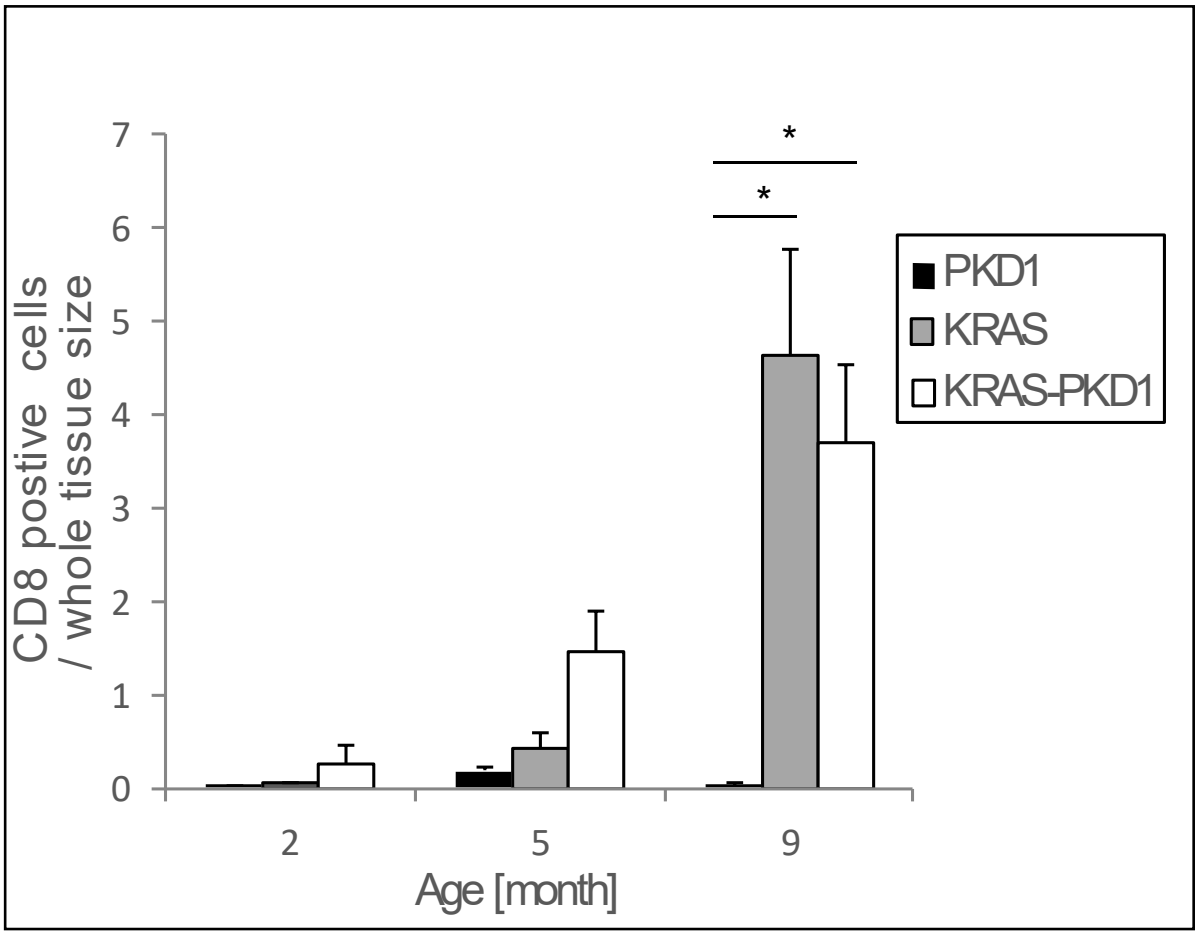

Figure 17: Infiltrating CD8$^+$ T-cell quantification

Graph shows the infiltration of CD8$^+$ T-cells. CD8$^+$ stained cells were counted and ratio to tissue size was calculated. 9-months-old p48-Cre-KRAS^{G12D} and p48-Cre-KRAS^{G12D}-PKD1$^{-/-}$mice show a significant infiltration of CD8$^+$ cells, whereby 5-months-old p48-Cre-KRAS^{G12D}-PKD1$^{-/-}$ mice indicate already an earlier influx of CD8$^+$ cells in pancreatic cancer tissues. But a high infiltration of CD8$^+$ cells were seen in pancreatic cancer samples. Bars represent mean values ± SEM of three different mouse lines and age groups; *P < 0.05.
KRAS: *p48-Cre-KRAS^{G12D};* ***PKD1:*** *p48-Cre-PKD1$^{-/-}$;* ***KRAS -PKD1:*** *p48-Cre-KRAS^{G12D}-PKD1$^{-/-}$*

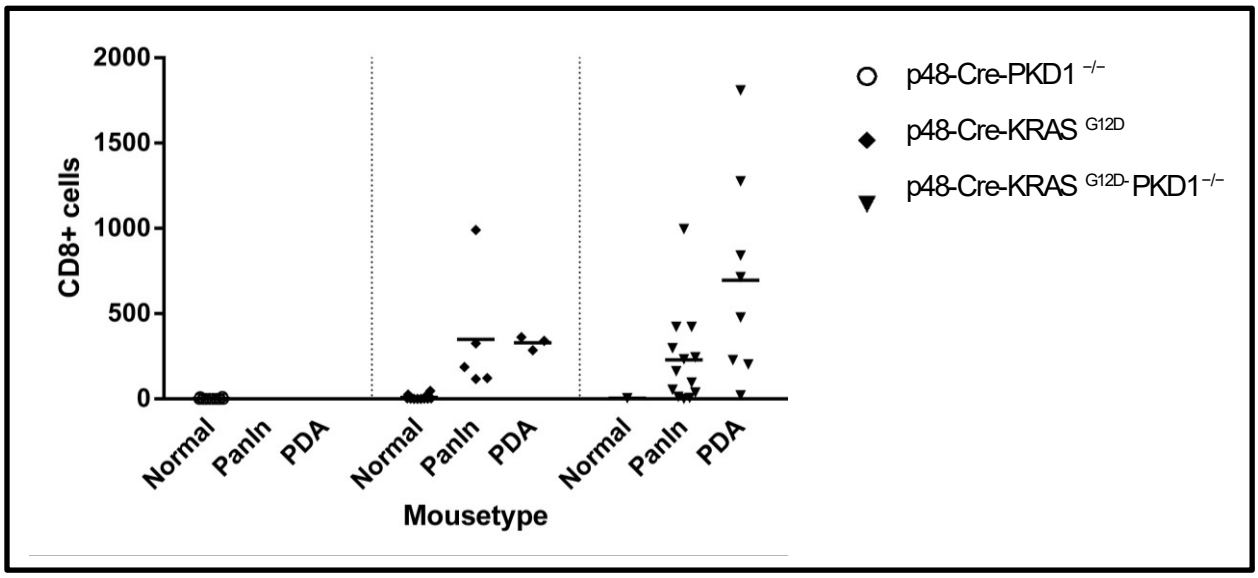

Figure 18: CD8$^+$ T-cell distribution by disease stage

Graph shows distribution of absolute CD8$^+$ cell amounts separated into different tumor levels: normal tissue, PanIN: pancreata which had not developed carcinoma yet and pancreata with Pancreatic ductal adenocarcinoma (PDC). We see an increased influx of CD8$^+$ T-cells in pancreatic cancer tissue of p48-Cre-KRAS^{G12D}-PKD1$^{-/-}$mice compared to PDC tissue of p48-Cre-KRAS^{G12D} mice. But Pancreatic intraepithelial neoplasia (PanIN) mice show fewer infiltrating cells in both groups.

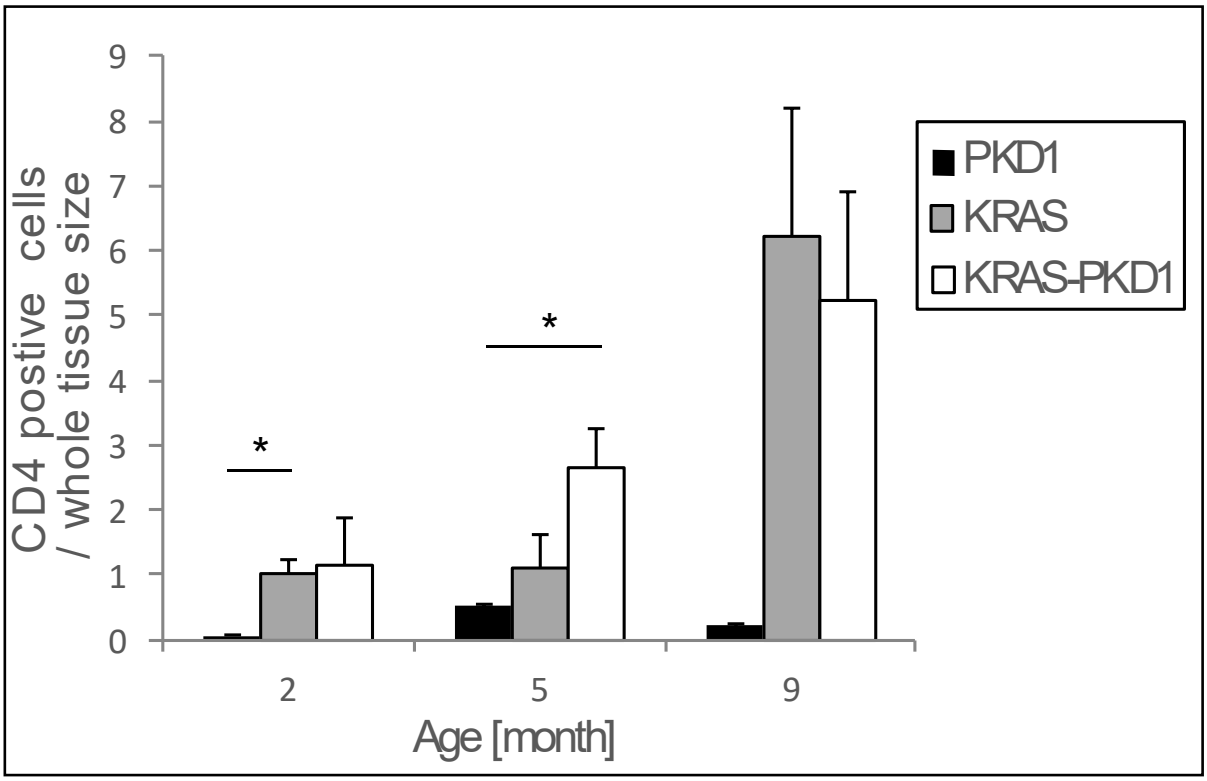

Figure 19: Infiltrating CD4$^+$ T-cell quantification

CD4$^+$ stained cells were counted and ratio to tissue size was calculated. 9-months-old p48-Cre-KRAS^{G12D} and p48-Cre-KRAS^{G12D}-PKD1$^{-/-}$ mice show a significant infiltration of CD4$^+$ cells. 5-months-old p48-Cre-KRAS^{G12D}-PKD1$^{-/-}$ mice show an earlier influx of CD4$^+$ T-cells. Bars represent mean values ± SEM of three different mouse lines and age groups; *P < 0.05.

KRAS: *p48-Cre-KRAS^{G12D};* ***PKD1:*** *p48-Cre-PKD1$^{-/-}$;* ***KRAS -PKD1:*** *p48-Cre-KRAS^{G12D}-PKD1$^{-/-}$*

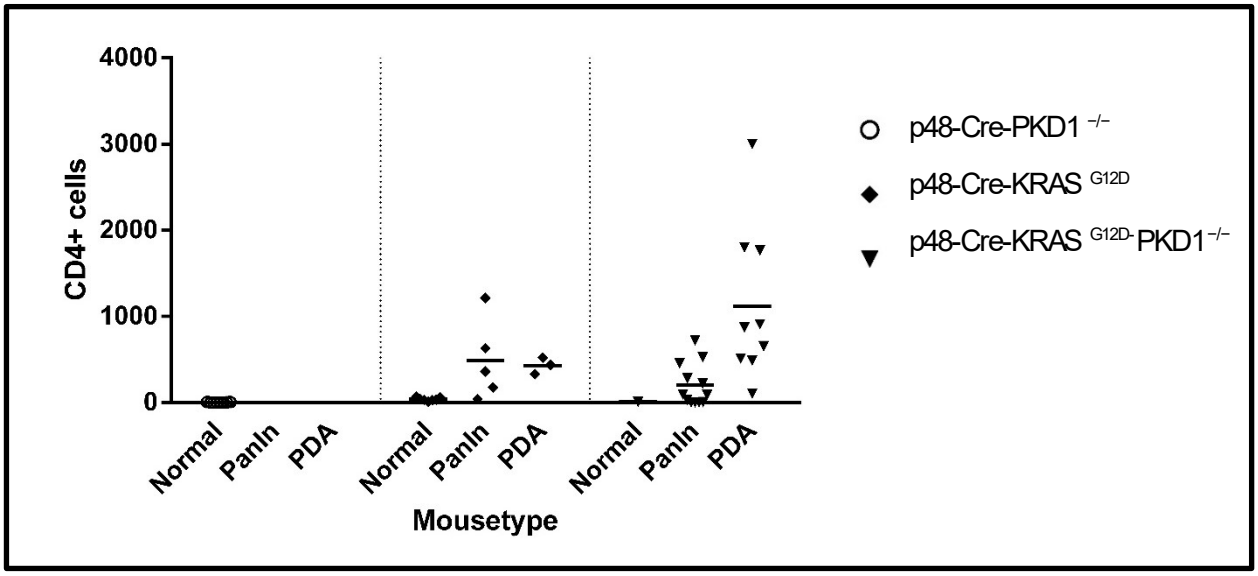

Figure 20: CD4$^+$ T-cell distribution, sorted by disease stage

Graph shows distribution of absolute CD4$^+$ cell amounts separated in different tumor levels: normal tissue, PanIN: pancreata which had not developed carcinoma yet and pancreata with Pancreatic ductal adenocarcinoma (PDC). Like CD8$^+$ cells, there is also an increased infiltration of CD4$^+$ cells in PDAC mice of p48-Cre-KRAS^{G12D}-PKD1$^{-/-}$ group compared to PDAC p48-Cre-KRAS^{G12D} mice. We see low CD4$^+$ T-cells in p48-Cre-KRAS^{G12D}-PKD1$^{-/-}$ mice as compared to PDAC p48-Cre-KRAS^{G12D}

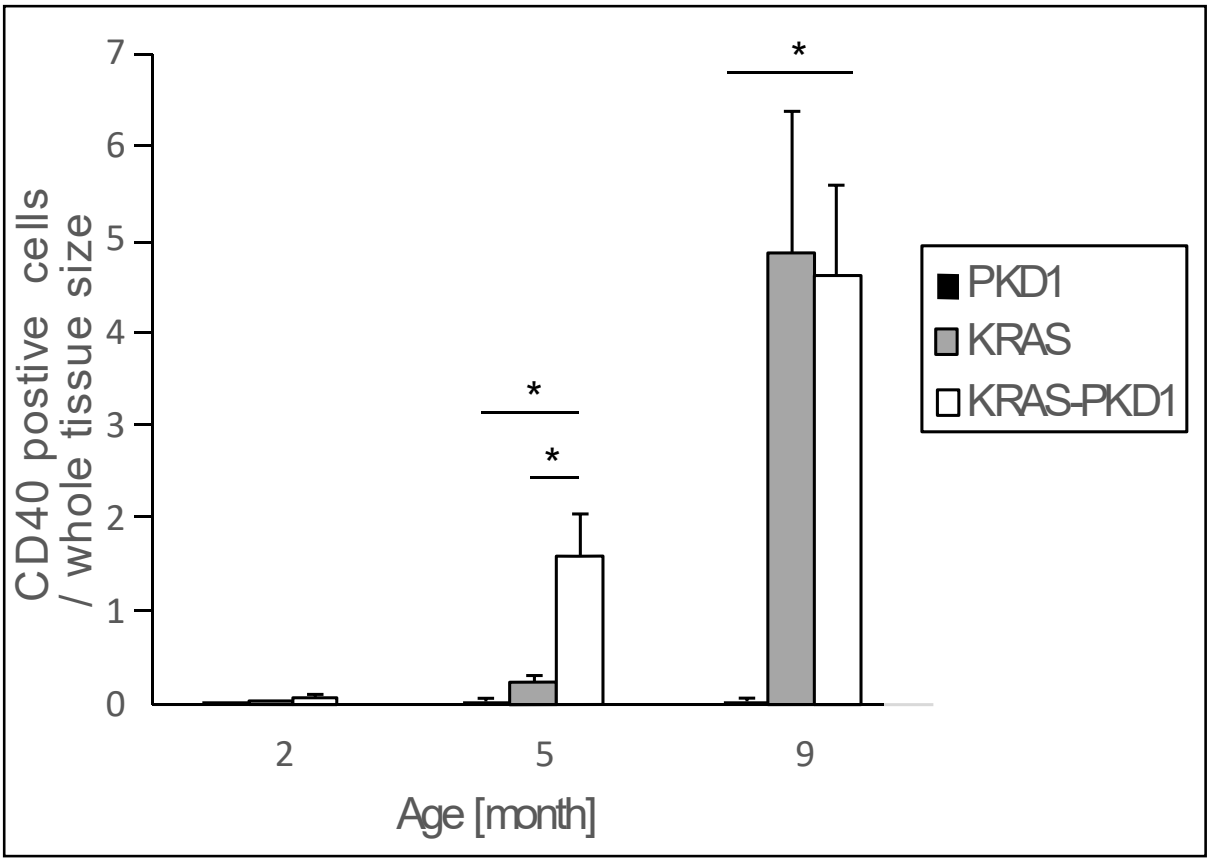

Figure 21: Infiltrating CD40$^+$ cell quantification

CD40$^+$ cells were counted and ratio to tissue size was calculated. CD40 cells are thought to regulate B- and T-cell proliferation. PKD1 knockout with concomitant KRAS mutation leads to early CD40$^+$ cell infiltration as compared to mice with only KRAS^{G12D}mutation. This increase is also positively correlated with tumor progression, as well as the influx of T-lymphocytes. Bars represent mean values ± SEM of three different mouse lines and age groups; *P < 0.05.

KRAS: *p48-Cre-KRAS^{G12D};* ***PKD1:*** *p48-Cre-PKD1$^{-/-}$;* ***KRAS -PKD1:*** *p48-Cre-KRAS^{G12D}-PKD1$^{-/-}$*

To complete the analysis of lymphocyte subtypes, we examined the infiltration of B220$^+$ B lymphocytes by IHC staining (Figure 22). 2-months-old animals in all three mouse groups do not show any significant B-cells. Beginning infiltration of pancreatic B cells are mainly observed in 5-months *p48-Cre-KRAS^{G12D}-PKD1$^{-/-}$* with increasing amounts at 9 months of age. *p48-Cre-KRAS^{G12D}* mice show significant higher amounts of B cells in pancreata of 9-months-old mice (Figure 23). They are often seen in stromal tissue around tissue and appear rather in larger groups and are seen around high level PanIN-3 lesions together with stromal tissue around.

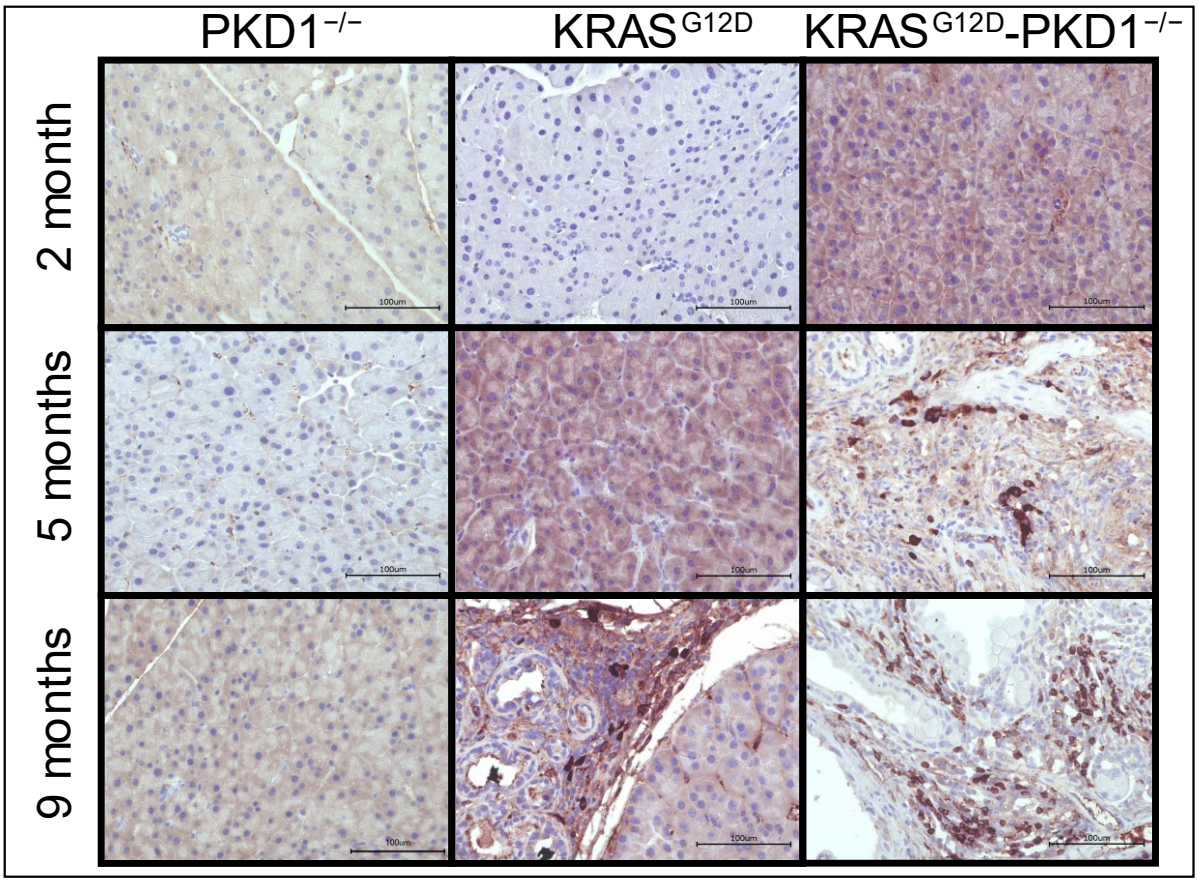

Figure 22: IHC staining for B-Lymphocytes

Representative pictures of B220^{+} cells in pancreas sections of three different mouse lines. B220^{+} is used to detect B-lymphocytes. Like other inflammatory cells, they also correlate with tumor progression (see Figure 23). Size bars indicate 100 µm. There is seen an early influx in PKD1 knockout mice with KRAS mutation at 5 months of age.

KRAS: *p48-Cre-KRAS^{G12D};* ***PKD1:*** *p48-Cre-PKD1$^{-/-}$;* ***KRAS -PKD1:*** *p48-Cre-KRAS^{G12D}-PKD1$^{-/-}$*

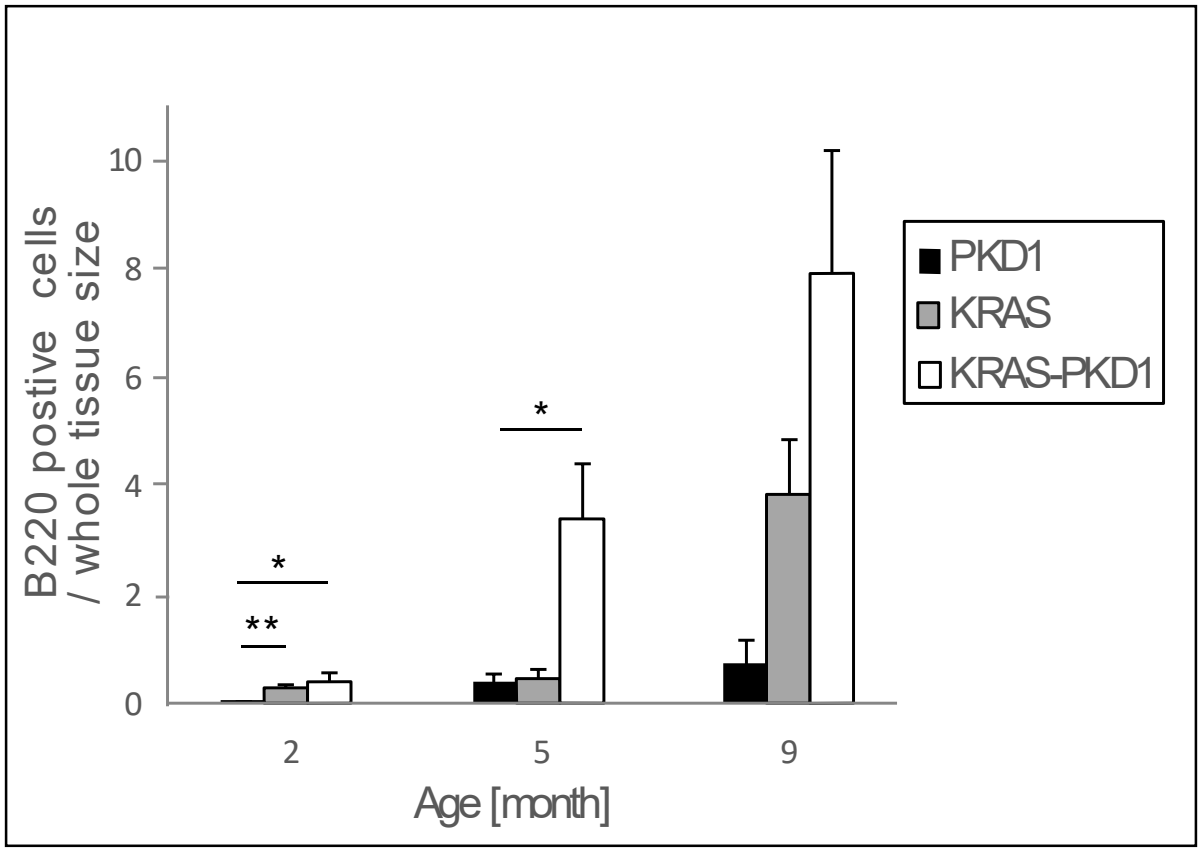

Figure 23: Infiltrating B-Lymphocyte quantification

Ratio of cells to tissue is calculated and visualized for B-Lymphocytes (B220^{+} cells). 5-months-old p48-Cre-KRAS^{G12D}-PKD1$^{-/-}$ mice show a significant number of B-Lymphocytes as compared to mice with only KRAS^{G12D} mutation. There is also seen a strong increase of those cells in 9-months-old animals, whereas p48-Cre-KRAS^{G12D} mice half as much cells. Like the other inflammatory cells, B-lymphocytes are positively correlating with tumor progression. Bars represent mean values ± SEM of three different mouse lines and age groups; *P < 0.05.

KRAS: *p48-Cre-KRAS^{G12D};* ***PKD1:*** *p48-Cre-PKD1$^{-/-}$;* ***KRAS-PKD1:*** *p48-Cre-KRAS^{G12D}-PKD1$^{-/-}$*

4. Discussion

Protein Kinase D1 (*PKD1*), a serine/threonine kinase, plays an essential role in several important cellular processes, including cytoskeletal reorganisation, exosome secretion, apoptosis, cell growth/migration and angiogenesis. However, possible therapeutic strategies targeting PKD1 in pancreatic ductal adenocarcinoma (PDCA) still remains an understudied area. In my doctoral thesis I studied the effect of a pancreatic-specific *Cre* mediated knockout of *PKD1* in an oncogenic *p48-KRAS*^{G12D} mouse model, a well-established model to study the initiation and development of pancreatic cancer *in vivo*. Interestingly, we observed a lower survival rate in early tumour stages in *p48-KRAS*^{G12D}-*PKD1*$^{-/-}$ mice (Figure 4 and 8). These findings suggest that *PKD1* plays an important role in pancreatic cancer progression. In these mice, we detected early desmoplastic reactions, characterized by rich fibrosis, ADM/PanIN lesions and infiltrating immune cells compared to the control groups (Figure 7, 8 and 11). When we scored the PanIN lesions, based on amount and severity, we observed a positive correlation with stromal deposits levels (as shown in Figure 7 and 9). We concluded a strong interaction between those pathologic structural changes and infiltrating of immune cells caused by *PKD1* loss. In order to better understand the function of *PKD1*, numerous studies were conducted in the last years. For instance, *PKD1* was studied in ductal breast cancer with its ductal nature like pancreatic precursor lesions. In 2009, Eiseler *et al.* have identified a decreased expression of *PKD1* in human invasive ductal breast cancer and high *PKD1* expression was detected in epithelial ductal tissue of healthy human breast samples (Eiseler *et al.* 2009). This study suggested that *PKD1* expression is decreased when cells achieve a more aggressive state in cancer. In addition, a clear tumor promoting effect of *PKD1* knockout in lower-invasive cells had been demonstrated (Eiseler *et al.* 2009). Furthermore, constitutively-active *PKD1* re-introduced in in mammary gland tumor drastically reduced their ability of tumor cells to invade in 2D and 3D cell culture (Eiseler *et al.* 2009). This described study was performed in breast cancer cells. So, there is a need to further analyze the effect of *PKD1* loss in PDAC. Further research is required to answer, how normal pancreatic and cancer cells interact with each other as well as the interaction with stromal components. In this context, we need to better understand the transdifferentiation process in PDAC, an important point in PDAC initiation.

Yet, how *PKD1* loss affects the transdifferentiation process is still not fully understood. In 2014, Wille *et al.* have described a cell proliferation enhancement function for *PKD1* in tumor cells (Wille *et al.* 2014). However, such an effect was not described for normal pancreatic tissue (Wille *et al.* 2014). Interestingly, we detected the same result in our healthy control mice. No

effect of *PKD1* loss without KRAS mutation was observed in our mouse model. These findings suggest that the tumour initiation process requires an additional oncogenic event like a *KRAS* activation. In addition, Wille *et al.* suggested an anti-invasiveness function for *PKD1* in pancreas tumour cells. These published findings explain the accelerated progression of PDAC in our *p48-KRAS*^{G12D}*-PKD1*$^{-/-}$ mouse model compared to our control *p48-KRAS*^{G12D} mice. We hypothesize that after initiation of desmoplastic changes caused by *KRAS* mutation, *PKD1* loss and/or tissue damage, provide the cells with an advantage to generate a high-migratory phenotype in late stages of disease. This is caused by control over actin-regulatory proteins such as cofilin-phosphatase slingshot-1L (SSH1L) (Eiseler *et al.* 2012; Wille *et al.* 2014). Furthermore, another isoform of the *PKD* family, *PKD2* was described in these studies as a pro-invasive phenotype by a massive upregulation of MMP7/9 (Wille *et al.* 2014). Thus, the opposing roles for *PKD1* and *PKD2* can elucidated the growth phenotype we observed in our mouse model: when we knockout *PKD1,* the anti-invasive role is diminished and the predominating function of *PKD2* is promoting invasion and angiogenesis (Wille *et al.* 2014). This can lead to an increase in PanIN/PDAC development. Nevertheless, our results did not show any early effects of *PKD1* loss and support for tumor initiation. Our findings proposed an interaction or effect of *PKD1* on cancer cells, mainly initiated by an oncogenic *KRAS* event. After initiation, *PKD1* loss accelerates tumor progression. One mechanism of this process was shown to be regulated by MMPs (Wille *et al.* 2014). It has been re-confirmed the anti-invasive effect of *PKD1* is mediated by its role as a regulator of expression and activity of invasion-relevant MMPs (Wille *et al.* 2014). Additionally, it has been described that MMP-7 and MMP-9 are positively regulated by *PKD2* (Wille *et al.* 2014). Our results emphasize the same tumor promoting mechanism: PKD functions as suppressor of MMPs and facilitates tumor migration and growth. *PKD1* negatively mediates cancer cell invasion mainly through the regulation of invasion-relevant MMP expressions, which is lost when *PKD1* is deleted (Eiseler *et al.* 2009). Subsequently, loss of *PKD1* increases *PKD2* downstream target expression (both MMP-7 and MMP-9) to promote tumor invasion and angiogenesis. Taken together, this data confirms a tumor-suppressing role of *PKD1* and the increase in tumor development in our *p48-KRAS*^{G12D}*-PKD1*$^{-/-}$ mouse model. Based on these data, there is urgent need for a selective PKD1 targeting drug to analyse its function without impairing PKD2 function. The regulation of MMPs by *PKD1* is not the only pathway to affect tumor progression.

Recently, it has been been proposed that loss of *PKD1* can contribute to cancer development via a previously unknown mechanism. *PKD1* has been shown to regulate cell function via

exosomes and loss of *PKD1* increased cell migration (Costa-Silva *et al.* 2015, Mazzeo *et al.* 2016). The tumor-derived exosomes contain various proteins, DNAs, and mRNAs that are able to induce local and metastatic spread of PDAC cells (Costa-Silva *et al.* 2015). Additionally, several published studies demonstrated that exosomes play an essential role in inflammation in tumor microenvironment (Wu *et al.* 2016). Furthermore, exosomes from gastric cancer cells activate the NF-κB signalling pathway, and thus increased pro-inflammatory factors. We hypothesized a similar mechanism in our PDCA mouse models. *PKD1* loss results in an increased cytoskeletal reorganisation with higher levels of cell migration and exosome secretion. In consequent, a developing inflammatory microenvironment lead to further progression of PDAC. Taken together, the deletion of *PKD1* in our *p48-KRAS*^{G12D}-*PKD1*$^{-/-}$mouse model leads to an increase in progressive PDAC phenotype. Most likely by upregulation of cell migration and exosome secretion. However, this hypothesis has to be further tested in follow-up studies.

Due to upregulation of inflammatory cytokines through exosomes and previously published studies, we anticipated an increase in infiltrating immune cells. In fact, in desmoplastic regions we detected different inflammatory cells, mainly macrophages and T-lymphocytes (Figure 14 and 16). Previous studies have shown the importance of inflammatory cells in initiation and progression of PDAC (Guerra *et al.* 2011; Guerra *et al.* 2007). In 2014, Wang *et al.* proposed that *PKD1* promotes oncogene-induced senescence by up-regulation of NF-κB that subsequently increases COX-2 activity (Wang *et al.* 2014). This leads to the hypothesis that *PKD1* knockout should lead to a decreased COX-2 activity in our *p48-KRAS*^{G12D}-*PKD1*$^{-/-}$ mouse model. However, our results did not support these previously published findings. The COX-2 activity is significantly increased in 5-months-old *p48-KRAS*^{G12D}-*PKD1*$^{-/-}$ mice compared to *p48-KRAS*^{G12D} mice (Figure 10). The activation of COX-2 can be explained by an increased exosome secretion mediated by the loss of *PKD1*, known to be caused by the activation of the NF-κB pathway (Hu *et al.* 2017). As a result of high COX-2 activation, angiogenesis is induced, that is known to promote tumor progression (Hu *et al.* 2017). Another promoting factor in PDAC progression besides inflammation is hypoxia (Zhang *et al.* 2018). Hypoxia is a key feature in high desmoplastic PDAC microenvironment that can induce inflammatory pathways by secretion of IL-1β. In 2018, Zhang *et al.* demonstrated that hepatocellular carcinoma tumor-associated macrophages (TAMs) secreted more interleukin IL-1β under moderate hypoxic conditions (Zhang *et al.* 2018). IL-1β is inducing COX-2 expression, which results in upregulation of hypoxia inducible factor 1α (Zhang *et al.* 2018).

This results in cancer cell epithelial–mesenchymal transition and metastasis that accelerates PanIN development (Zhang *et al.* 2018). Both conditions, hypoxia and TAMs infiltration are present in PDAC as well. For that reason, we hypothesize a comparable mechanism for inflammation in our PDAC mouse models.

Inflammatory reactions *in vivo* lead to immune cell infiltrations, mainly in PDAC developing mice (Figure 12). We observed a significant increase in macrophages and T-lymphocytes infiltration as dominating immune cells population in *p48-KRAS*^{G12D}*-PKD1*$^{-/-}$ mice (Figure 14 and 16). Both cell types are known to be activated by NF-κB. Furthermore, the origin of TAMs, monocyte-derived or tissue-resident macrophages, is a subject that gained intense focus in research lately (Zhu *et al.* 2017). Interestingly, Zhu *et al.* report that activated KRAS signalling activates tissue-resident macrophages and promotes an inflammatory environment within PDAC (Zhu *et al.* 2017). When we analyzed *p48-KRAS*^{G12D}*-PKD1*$^{-/-}$ mouse model, we detected an early infiltration of macrophages with a subsequent fibrogenesis development. For that reason, we hypothesized that a M1 to M2 polarisation of TAMs in our mouse model promotes fibrogenesis and induces leucocyte infiltration. It is been reported previously that the polarisation of TAMs from M1 to M2 phenotype is initiated by cytokine signals, including IL-10 and TGF-β, received from T_{reg} and pancreatic tumor cells (Sica and Mantovani 2012). The M2 macrophages have been associated with promoting an immunosuppressive state of tumor microenvironment by production various mediators that support fibrogenesis and tissue invasion mainly through the release of MMPs and collagens (Ostrand-Rosenberg *et al.* 2012; Ruffell, Affara and Coussens 2012; Zhu *et al.* 2017). It is considered that the prevention or inversion of a M2 polarization can be proposed as a therapy option. Therefore, it is of important that we have to conduct more research to further analyze the TAM subtypes in our PDAC mouse models. But so far, a direct regulation of macrophages by *PKD1* is not described yet. For that reason, we hypothesize an indirect activation and attraction of TAMs in PDAC as described above.

In addition, it has been suggested that CD40 is promoting macrophage activation and infiltration (Beatty *et al.* 2011). $CD40^{+}$ cells are detected in 5-months-old *p48-KRAS*^{G12D}*-PKD1*$^{-/-}$ mice compared to their littermates (Figure 21) (Beatty *et al.* 2011). In 2011, Beatty *et al.* suggested that CD40-activated TAMs are capable of degrading stromal tissue in PDAC without T-lymphocyte effectors (Beatty *et al.* 2011). An activation of CD40 expressing TAMs can lead to an inversion of macrophages to an M1 phenotype to restore tumor immune surveillance (van Attekum *et al.* 2017). However, our results support the hypothesis, that TAMs in PDAC are

mainly M2 phenotypes, therefore immunosuppressive (Ruffell, Affara and Coussens 2012; Ostrand-Rosenberg *et al.* 2012). For that reason, a therapeutic possibility has to be tested in future of inversion of macrophages from M1 to M2 phenotype. CD40 activation and its effect on stromal degrading is T-lymphocyte independent (Beatty *et al.* 2011). But T-lymphocytes were the most prominent inflammatory cell population in stromal regions together with macrophages. Another important player for anti-tumor effect are $CD8^+$ T-lymphocytes (Clark *et al.* 2007). They are reported to be low in pancreatic cancer, whereas $CD4^+$ cells, especially T_{reg} cells and Th_2 cells have been reported to be increased in pancreatic cancer (Clark *et al.* 2007). We showed an increase of T-lymphocyte ($CD4^+$ and $CD8^+$ cells) infiltration, correlating with increasing carcinoma level in PDAC (Figure 18 and 20). However, the T-lymphocyte infiltration was limited to fibrotic areas without having contact to cancer cells. This observation emphasizes the fact, that stromal tissue is preventing pancreatic carcinoma from anti-tumor function of the immune system. Furthermore, Clark *et al.* have described an inactivity of T-lymphocytes in PDAC, so that we suspect the same fact for T-lymphocytes in our PDAC mouse model (Clark *et al.* 2007). Knowing that published data, it has to be tested whether T-lymphocytes in our PDAC mouse models are functioning or are inactive. And for further therapeutic strategies as anti-tumor cells, $CD8^+$ cells have to be attracted to tumor cells. The same situation is observed for $CD4^+$ cells. In our PDAC mice, $CD4^+$ cells are confined in the stromal tissue. $CD4^+$ cells can differentiate into Th_1, Th_2, Th_{17} and T_{reg} subpopulations with different distinct functions (Gagliani et al. 2017). T_{reg} cells and macrophages are linked to tumor promotion and tumor immune suppression (Josefowicz *et al.* 2012). So, there are more studies needed to better understand the function of T_{reg} cells in PDAC. In a recent study by Lunardi *et al.*, it has been shown that Pancreatic stellate cells (PSCs) are able to express IP-10 to recruit T_{reg} cells (Lunardi *et al.* 2014). Therefore, the progressively increasing stromal tissue with abundant PSCs can be presumed as an additional promoting factor for T_{reg} recruitment. However, to test this hypothesis more studies on pancreatic cancer tissue with more precise techniques to identify the subpopulation of $CD4^+$ T-cell, the localisations and functionality within the tumor have to be conducted. In summary, T-Lymphocytes and macrophages play an important role in PDAC development, both as activator or suppressor of cancer progression. For therapeutic strategies, activating tumor supressing lymphocytes and macrophages have to be identified. Another potential problem will be to bring these effector cells to tumor side by degrading stromal tissue known to block the migration.

In conclusion, loss of *PKD1* leads to a significant earlier onset of tumor development in the presence of an oncogenic $KRAS^{G12D}$ gene. Our results demonstrated that *PKD1* is involved in

cell interactions between various cell types, such as cancer cells and inflammatory cells. In addition, we showed that *PKD1* is an important factor in controlling and balancing inflammatory reactions by taking part directly or indirectly in inflammatory pathways. All these results suggest a tumor promoting function of *PKD1* loss/downregulation.

5. Summary

The aim of my doctoral thesis was to characterize the effect of Protein Kinase D1 (*PKD1)* loss in an oncogenic *KRAS*^{G12D}-driven genetic mouse model of pancreatic cancer *in vivo*. To obtain first insights we focused on tumor and desmoplastic development and analyzed immune cell infiltration. We evaluated three mouse lines (*p48-KRAS*^{G12D}, *p48-KRAS*^{G12D}*-PKD1*$^{-/-}$ and *p48-PKD1*$^{-/-}$) for cancer progression over a period of one year and detected a significant reduction of overall survival in *p48-KRAS*^{G12D}*-PKD1*$^{-/-}$ mice compared to control littermates. We detected a significant increase in progressive Pancreatic intraepithelial neoplasias (PanIN) and collagen deposit development at 2, 5, and 9 months of analysis. We discovered that *p48-KRAS*^{G12D}*-PKD1*$^{-/-}$ mice at the age of 5 month developed early precursor PanIN lesion, while aged-matched controls *p48-KRAS*^{G12D} and *p48 -PKD1*$^{-/-}$ mice had no sign of precursor PanIN lesion. In addition, we firmly demonstrated that the pancreas cancer development is associated with an increase in desmoplastic reaction (collagen deposit) and leucocyte infiltration. However, the molecular mechanism of *PKD1* role in stromal tissue remains unclear. Here, we have demonstrated that *PKD1*-deficiency accelerates tumor development in an oncogenic KRAS mouse model (*p48-KRAS*^{G12D}*-PKD1*$^{-/-}$) *in vivo*. We hypothesize that cancer cells and stromal cell interact and promote immune cell infiltration to the desmoplastic field *in vivo*. Our findings raised further interesting open questions, e.g. the cellular interaction of cancer cells and stromal cells at a molecular level.

Taken together, our data suggest that *PKD1* has a tumor supressing function in Pancreatic ductal adenocarcinoma (PDAC), in particular at early disease stages. *PKD1* loss in an oncogenic KRAS background results in a significantly earlier and faster initiation of Acinar-to-ductal metaplasias (ADMs) and PanINs. These *PKD1*-deficient tumors showed an increased inflammatory reaction and accelerated infiltration of leucocytes that accelerates cancer progression. The key immune cell populations that we detected in PDAC were macrophages and T-lymphocytes. Overall, our data demonstrated that *PKD1* plays an essential role in pancreatic cancer progression *in vivo*. Our novel findings are thus not only of scientific relevance, but also of potentially clinical relevance.

6. References

1. Ahrens, D. von, Bhagat, T. D., Nagrath, D., Maitra, A., & Verma, A. The role of stromal cancer-associated fibroblasts in pancreatic cancer. Journal of hematology & oncology 10: 76 (Review) (2017)
2. Azoitei, N., Pusapati, G. V., Kleger, A., Möller, P., Küfer, R., Genze, F., Wagner, M., van Lint, J., Carmeliet, P., Adler, G., & Seufferlein, T. Protein kinase D2 is a crucial regulator of tumour cell-endothelial cell communication in gastrointestinal tumours. Gut 59: 1316–1330 (2010)
3. Basturk O, Hong SM, Wood LD, Adsay NV, Albores-Saavedra J, Biankin AV, Brosens LA, Fukushima N, Goggins M, Hruban RH, Kato Y, Klimstra DS, Klöppel G, Krasinskas A, Longnecker DS, Matthaei H, Offerhaus GJ, Shimizu M, Takaori K, Terris B, Yachida S, Esposito I, Furukawa T. A Revised Classification System and Recommendations from the Baltimore Consensus Meeting for Neoplastic Precursor Lesions in the Pancreas. The American journal of surgical pathology 39: 1730–1741 (2015)
4. Banerjee K, Kumar S, Ross KA, Gautam S, Poelaert B, Nasser MW, Aithal A, Bhatia R, Wannemuehler MJ, Narasimhan B, Solheim JC, Batra SK, Jain M. Emerging trends in the immunotherapy of pancreatic cancer. Cancer letters 417: 35–46 (2018)
5. Beatty, G. L., Chiorean, E. G., Fishman, M. P., Saboury, B., Teitelbaum, U. R., Sun, W., Huhn, R. D., Song, W., Li, D., Sharp, L. L., Torigian, D. A., O'Dwyer, P. J., & Vonderheide, R. H. CD40 agonists alter tumor stroma and show efficacy against pancreatic carcinoma in mice and humans. Science (New York, N.Y.) 331: 1612–1616 (2011)
6. Beatty, G. L., Li, Y., & Long, K. B. Cancer immunotherapy: activating innate and adaptive immunity through CD40 agonists. Expert review of anticancer therapy 17: 175–186 (2017)
7. Biankin AV, Waddell N, Kassahn KS, Gingras MC, Muthuswamy LB, Johns AL, Miller DK, Wilson PJ, Patch AM, Wu J, Chang DK, Cowley MJ, Gardiner BB, Song S, Harliwong I, Idrisoglu S, Nourse C, Nourbakhsh E, Manning S, Wani S, Gongora M, Pajic M, Scarlett CJ, Gill AJ, Pinho AV, Rooman I, Anderson M, Holmes O, Leonard C, Taylor D, Wood S, Xu Q, Nones K, Fink JL, Christ A, Bruxner T, Cloonan N, Kolle G, Newell F, Pinese M, Mead RS, Humphris JL, Kaplan W, Jones MD, Colvin EK, Nagrial AM, Humphrey ES, Chou A, Chin VT, Chantrill LA, Mawson A, Samra JS, Kench JG, Lovell JA, Daly RJ, Merrett ND, Toon C, Epari K, Nguyen NQ, Barbour A, Zeps N; Australian Pancreatic Cancer Genome Initiative, Kakkar N, Zhao F, Wu YQ, Wang M, Muzny DM, Fisher WE, Brunicardi FC, Hodges SE, Reid JG, Drummond J, Chang K, Han Y, Lewis LR, Dinh H, Buhay CJ, Beck T, Timms L, Sam M, Begley K, Brown A, Pai D, Panchal A, Buchner N, De Borja R, Denroche RE, Yung CK, Serra S, Onetto N, Mukhopadhyay D, Tsao MS, Shaw PA, Petersen GM, Gallinger S, Hruban RH, Maitra A, Iacobuzio-Donahue CA, Schulick RD, Wolfgang CL, Morgan RA, Lawlor RT, Capelli P, Corbo V, Scardoni M, Tortora G, Tempero MA, Mann KM, Jenkins NA, Perez-Mancera PA, Adams DJ, Largaespada DA, Wessels LF, Rust AG, Stein LD, Tuveson DA, Copeland NG, Musgrove

EA, Scarpa A, Eshleman JR, Hudson TJ, Sutherland RL, Wheeler DA, Pearson JV, McPherson JD, Gibbs RA, Grimmond SM. Pancreatic cancer genomes reveal aberrations in axon guidance pathway genes. Nature 491(7424): 399–405 (2012)

8. Clark, C. E., Hingorani, S. R., Mick, R., Combs, C., Tuveson, D. A. & Vonderheide, R. H. Dynamics of the immune reaction to pancreatic cancer from inception to invasion. Cancer research 67: 9518–9527 (2007)
9. Costa-Silva B, Aiello NM, Ocean AJ, Singh S, Zhang H, Thakur BK, Becker A, Hoshino A, Mark MT, Molina H, Xiang J, Zhang T, Theilen TM, García-Santos G, Williams C, Ararso Y, Huang Y, Rodrigues G, Shen TL, Labori KJ, Lothe IM, Kure EH, Hernandez J, Doussot A, Ebbesen SH, Grandgenett PM, Hollingsworth MA, Jain M, Mallya K, Batra SK, Jarnagin WR, Schwartz RE, Matei I, Peinado H, Stanger BZ, Bromberg J, Lyden D. Pancreatic cancer exosomes initiate pre-metastatic niche formation in the liver. Nat Cell Biol 17: 816-26 (2015)
10. De Monte L, Wörmann S, Brunetto E, Heltai S, Magliacane G, Reni M, Paganoni AM, Recalde H, Mondino A, Falconi M, Aleotti F, Balzano G, Algül H, Doglioni C, Protti MP. Basophil Recruitment into Tumor-Draining Lymph Nodes Correlates with Th2 Inflammation and Reduced Survival in Pancreatic Cancer Patients. Cancer research 76: 1792–1803 (2016)
11. Distler M, Aust D, Weitz J, Pilarsky C, Grutzmann R. Precursor lesions for sporadic pancreatic cancer: PanIN, IPMN, and MCN. Biomed Res Int 2014: 474905 (Review) (2014)
12. Eiseler, T., Doppler, H., Yan, I. K., Goodison, S., & Storz, P. Protein kinase D1 regulates matrix metalloproteinase expression and inhibits breast cancer cell invasion. Breast cancer research 11: R13 (2009)
13. Eiseler T, Köhler C, Nimmagadda SC, Jamali A, Funk N, Joodi G, Storz P, Seufferlein T. Protein kinase D1 mediates anchorage-dependent and -independent growth of tumor cells via the zinc finger transcription factor Snail1. The Journal of biological chemistry 287: 32367–32380 (2012)
14. Fielitz J, Kim MS, Shelton JM, Qi X, Hill JA, Richardson JA, Bassel-Duby R, Olson EN. Requirement of protein kinase D1 for pathological cardiac remodeling. Proceedings of the National Academy of Sciences of the United States of America 105(8): 3059–3063 (2008)
15. Gagliani, N., & Huber, S. Basic Aspects of T Helper Cell Differentiation. Methods in molecular biology 1514: 19–30 (2017)
16. Grant RC, Selander I, Connor AA, Selvarajah S, Borgida A, Briollais L, Petersen GM, Lerner-Ellis J, Holter S, Gallinger S. Prevalence of germline mutations in cancer predisposition genes in patients with pancreatic cancer. Gastroenterology 148: 556–564 (2015)
17. Greer, R. L., Staley, B. K., Liou, A., & Hebrok, M. Numb regulates acinar cell dedifferentiation and survival during pancreatic damage and acinar-to-ductal metaplasia. Gastroenterology 145: 1088-1097 (2013)

18. Guerra C, Schuhmacher AJ, Cañamero M, Grippo PJ, Verdaguer L, Pérez-Gallego L, Dubus P, Sandgren EP, Barbacid M. Chronic pancreatitis is essential for induction of pancreatic ductal adenocarcinoma by K-Ras oncogenes in adult mice. Cancer Cell 11: 291–302 (2007).
19. Guerra C, Collado M, Navas C, Schuhmacher AJ, Hernández-Porras I, Cañamero M, Rodriguez-Justo M, Serrano M, Barbacid M. Pancreatitis-induced inflammation contributes to pancreatic cancer by inhibiting oncogene-induced senescence. Cancer Cell 19: 728–739 (2011)
20. Guha, S., Tanasanvimon, S., Sinnett-Smith, J., & Rozengurt, E. Role of protein kinase D signaling in pancreatic cancer. Biochemical pharmacology 80: 1946–1954 (2010)
21. Habisch H, Zhou S, Siech M, Bachem MG. Interaction of stellate cells with pancreatic carcinoma cells. Cancers (Basel) 2: 1661-1682 (2010)
22. Hagemann T, Lawrence T, McNeish I, Charles KA, Kulbe H, Thompson RG, Robinson SC, Balkwill FR. "Re-educating" tumor-associated macrophages by targeting NF-kappaB. The Journal of experimental medicine 205: 1261–1268 (2008)
23. Hammel P, Huguet F, van Laethem JL, Goldstein D, Glimelius B, Artru P, Borbath I, Bouché O, Shannon J, André T, Mineur L, Chibaudel B, Bonnetain F, Louvet C; LAP07 Trial Group. Effect of Chemoradiotherapy vs Chemotherapy on Survival in Patients with Locally Advanced Pancreatic Cancer Controlled After 4 Months of Gemcitabine With or Without Erlotinib: The LAP07 Randomized Clinical Trial. JAMA, 315: 1844–1853 (2016)
24. Harikumar KB, Kunnumakkara AB, Ochi N, Tong Z, Deorukhkar A, Sung B, Kelland L, Jamieson S, Sutherland R, Raynham T, Charles M, Bagherzadeh A, Foxton C, Boakes A, Farooq M, Maru D, Diagaradjane P, Matsuo Y, Sinnett-Smith J, Gelovani J, Krishnan S, Aggarwal BB, Rozengurt E, Ireson CR, Guha S. A novel small-molecule inhibitor of protein kinase D blocks pancreatic cancer growth in vitro and in vivo. Molecular cancer therapeutics 9: 1136–1146 (2010)
25. He, P., Yang, J. W., Yang, V. W., & Bialkowska, A. B. Kruppel-like Factor 5, Increased in Pancreatic Ductal Adenocarcinoma, Promotes Proliferation, Acinar-to-Ductal Metaplasia, Pancreatic Intraepithelial Neoplasia, and Tumor Growth in Mice. Gastroenterology 154: 1494-1508 (2018)
26. Hingorani SR, Petricoin EF, Maitra A, Rajapakse V, King C, Jacobetz MA, Ross S, Conrads TP, Veenstra TD, Hitt BA, Kawaguchi Y, Johann D, Liotta LA, Crawford HC, Putt ME, Jacks T, Wright CV, Hruban RH, Lowy AM, Tuveson DA. Preinvasive and invasive ductal pancreatic cancer and its early detection in the mouse. Cancer Cell 4: 437–450 (2003)
27. Hingorani SR, Wang L, Multani AS, Combs C, Deramaudt TB, Hruban RH, Rustgi AK, Chang S, Tuveson DA. Trp53R172H and KrasG12D cooperate to promote chromosomal instability and widely metastatic pancreatic ductal adenocarcinoma in mice. Cancer Cell 7: 469–83 (2005)

28. Hu H., T. Han, M. Zhuo, L. Wu, C. Yuan, L. Wu, W. Lei, F. Jiao, and L.-W. Wang. Elevated COX-2 Expression Promotes Angiogenesis Through EGFR/p38-MAPK/Sp1-Dependent Signalling in Pancreatic Cancer. Sci Rep 7: 470 (2017)
29. Jang J-E, Hajdu CH, Liot C, Miller G, Dustin ML, Bar-Sagi D. Crosstalk between Regulatory T Cells and Tumor-Associated Dendritic Cells Negates Anti-tumor Immunity in Pancreatic Cancer. Cell Rep 20: 558-571 (2017)
30. Jackson EL, Willis N, Mercer K, Bronson RT, Crowley D, Montoya R, Jacks T, Tuveson DA. Analysis of lung tumor initiation and progression using conditional expression of oncogenic K-ras. Genes & development 15: 3243–3248 (2001)
31. Joshi NS, Akama-Garren EH, Lu Y, Lee DY, Chang GP, Li A, DuPage M, Tammela T, Kerper NR, Farago AF, Robbins R, Crowley DM, Bronson RT, Jacks T. Regulatory T Cells in Tumor-Associated Tertiary Lymphoid Structures Suppress Anti-tumor T Cell Responses. Immunity 43: 579–590 (2015)
32. Kamisawa T, Wood LD, Itoi T, Takaori K. Pancreatic cancer. Lancet 388(10039): 73-85 (2016)
33. Kawaguchi, Y., Cooper, B., Gannon, M., Ray, M., MacDonald, R. J., & Wright, C. V. E. The role of the transcriptional regulator Ptf1a in converting intestinal to pancreatic progenitors. Nature genetics 32: 128–134 (2002)
34. Kim MP, Evans DB, Wang H, Abbruzzese JL, Fleming JB, Gallick GE. Generation of orthotopic and heterotopic human pancreatic cancer xenografts in immunodeficient mice. Nat Protoc 4: 1670-1680 (2009)
35. Kirkegard, J., Mortensen, F. V., & Cronin-Fenton, D. Chronic Pancreatitis and Pancreatic Cancer Risk: A Systematic Review and Meta-analysis 112: 1366-1372 (2017)
36. Liou GY, Döppler H, Necela B, Krishna M, Crawford HC, Raimondo M, Storz P. Macrophage-secreted cytokines drive pancreatic acinar-to-ductal metaplasia through NF-κB and MMPs. The Journal of cell biology 202: 563–577 (2013)
37. Liou GY, Döppler H, Braun UB, Panayiotou R, Scotti Buzhardt M, Radisky DC, Crawford HC, Fields AP, Murray NR, Wang QJ, Leitges M, Storz P. Protein kinase D1 drives pancreatic acinar cell reprogramming and progression to intraepithelial neoplasia. Nature communications 6: 6200 (2015)
38. Luheshi, N., Davies, G., Poon, E., Wiggins, K., McCourt, M., & Legg, J. Th1 cytokines are more effective than Th2 cytokines at licensing anti-tumour functions in CD40-activated human macrophages in vitro. European journal of immunology 44: 162–172 (2014)
39. Lunardi S, Jamieson NB, Lim SY, Griffiths KL, Carvalho-Gaspar M, Al-Assar O, Yameen S, Carter RC, McKay CJ, Spoletini G, D'Ugo S, Silva MA, Sansom OJ, Janssen KP, Muschel RJ, Brunner TB. IP-10/CXCL10 induction in human pancreatic cancer stroma influences lymphocytes recruitment and correlates with poor survival. Oncotarget 5: 11064–11080 (2014)

40. Mazzeo, C.; Calvo, V.; Alonso, R.; Merida, I.; Izquierdo, M. Protein kinase D1/2 is involved in the maturation of multivesicular bodies and secretion of exosomes in T and B lymphocytes. Cell death and differentiation 23: 99–109 (2016)
41. Melstrom, L. G., Salazar, M. D., & Diamond, D. J. The pancreatic cancer microenvironment: A true double agent. Journal of surgical oncology 116: 7–15 (2017)
42. Muranaka T, Kuwatani M, Komatsu Y, Sawada K, Nakatsumi H, Kawamoto Y, Yuki S, Kubota Y, Kubo K, Kawahata S, Kawakubo K, Kawakami H, Sakamoto N. Comparison of efficacy and toxicity of FOLFIRINOX and gemcitabine with nab-paclitaxel in unresectable pancreatic cancer. Journal of gastrointestinal oncology 8: 566-571 (2017)
43. Murtaugh, L. C., & Leach, S. D. A case of mistaken identity? Nonductal origins of pancreatic "ductal" cancers. Cancer Cell 11: 211–213 (2007)
44. Neesse A, Bauer CA, Öhlund D, Lauth M, Buchholz M, Michl P, Tuveson DA, Gress TM. Stromal biology and therapy in pancreatic cancer. Gut 68: 861–868 (2011)
45. Ochi N, Tanasanvimon S, Matsuo Y, Tong Z, Sung B, Aggarwal BB, Sinnett-Smith J, Rozengurt E, Guha S. Protein kinase D1 promotes anchorage-independent growth, invasion, and angiogenesis by human pancreatic cancer cells. Journal of cellular physiology 226: 1074–1081 (2011)
46. Öhlund D, Handly-Santana A, Biffi G, Elyada E, Almeida AS, Ponz-Sarvise M, Corbo V, Oni TE, Hearn SA, Lee EJ, Chio II, Hwang CI, Tiriac H, Baker LA, Engle DD, Feig C, Kultti A, Egeblad M, Fearon DT, Crawford JM, Clevers H, Park Y, Tuveson DA. Distinct populations of inflammatory fibroblasts and myofibroblasts in pancreatic cancer. The Journal of experimental medicine 214: 579–596 (2017)
47. Peterburs, P., Heering, J., Link, G., Pfizenmaier, K., Olayioye, M. A., & Hausser, A. Protein kinase D regulates cell migration by direct phosphorylation of the cofilin phosphatase slingshot 1 like. Cancer research 69: 5634–5638 (2009)
48. Pomianowska E, Schjølberg AR, Clausen OPF, Gladhaug IP. COX-2 overexpression in resected pancreatic head adenocarcinomas correlates with favourable prognosis. BMC Cancer 14: 458 (2014)
49. Porzner, M., & Seufferlein, T. Novel approaches to target pancreatic cancer. Current cancer drug targets 11: 698–713 (2011)
50. Ren B, Liu X, Suriawinata AA. Pancreatic Ductal Adenocarcinoma and Its Precursor Lesions: Histopathology, Cytopathology, and Molecular Pathology. Am J Pathol 189: 9-21 (2019)
51. Roy A, Ye J, Deng F, Wang QJ. Protein kinase D signaling in cancer: A friend or foe? Biochim Biophys Acta Rev Cancer 1868: 283-294 (2017)
52. Ruffell, B., Affara, N. I., & Coussens, L. M. Differential macrophage programming in the tumor microenvironment. Trends in immunology 33: 119–126 (2012)
53. Seimiya T, Otsuka M, Iwata T, Tanaka E, Suzuki T, Sekiba K, Yamagami M, Ishibashi R, Koike K. Inflammation and de-differentiation in pancreatic carcinogenesis. World J Clin cases 6: 882-891 (2018)

54. Sica, A., & Mantovani, A. Macrophage plasticity and polarization: in vivo veritas. The Journal of clinical investigation 122: 787–795 (2012)
55. Siegel, R. L., Miller, K. D. & Jemal, A. Cancer Statistics, 2017. CA: a cancer journal for clinicians 67: 7–30 (2017)
56. Tang Y, Xu X, Guo S, Zhang C, Tang Y, Tian Y, Ni B, Lu B, Wang H. An increased abundance of tumor-infiltrating regulatory T cells is correlated with the progression and prognosis of pancreatic ductal adenocarcinoma. PLoS One 9: e91551 (2017)
57. van Attekum MHA, van Bruggen JAC, Slinger E, Lebre MC, Reinen E, Kersting S, Eldering E, Kater AP. CD40 signaling instructs chronic lymphocytic leukemia cells to attract monocytes via the CCR2 axis. Haematologica 102: 2069–2076 (2017)
58. Vincent, A., Herman, J., Schulick, R., Hruban, R. H., & Goggins, M. Pancreatic cancer. The Lancet 378: 607–620 (2011)
59. Wang P, Han L, Shen H, Wang P, Lv C, Zhao G, Niu J, Xue L, Wang QJ, Tong T, Chen J. Protein kinase D1 is essential for Ras-induced senescence and tumor suppression by regulating senescence-associated inflammation. Proceedings of the National Academy of Sciences of the United States of America 111: 7683–7688 (2014)
60. Wehr, A. Y., Furth, E. E., Sangar, V., Blair, I. A., & Yu, K. H. Analysis of the human pancreatic stellate cell secreted proteome. Pancreas 40: 557–566 (2011)
61. Wille C, Köhler C, Armacki M, Jamali A, Gössele U, Pfizenmaier K, Seufferlein T, Eiseler T. Protein kinase D2 induces invasion of pancreatic cancer cells by regulating matrix metalloproteinases. Molecular biology of the cell 25: 324–336 (2014)
62. Wille, C., Seufferlein, T. & Eiseler, T. Protein Kinase D family kinases: roads start to segregate. Bioarchitecture 4: 111–115 (2014)
63. Wu L, Zhang X, Zhang B, Shi H, Yuan X, Sun Y, Pan Z, Qian H, Xu W. Exosomes derived from gastric cancer cells activate NF-kappaB pathway in macrophages to promote cancer progression. In: Tumour biology: the journal of the International Society for Oncodevelopmental Biology and Medicine 37: 12169–12180 (2016)
64. Yamaguchi, J., Yokoyama, Y., Kokuryo, T., Ebata, T. & Nagino, M. Cells of origin of pancreatic neoplasms. Surgery today 48: 9–17 (2018)
65. Zhang J, Zhang Q, Lou Y, Fu Q, Chen Q, Wei T, Yang J, Tang J, Wang J, Chen Y, Zhang X, Zhang J, Bai X, Liang T. Hypoxia-inducible factor-1alpha/interleukin-1beta signaling enhances hepatoma epithelial-mesenchymal transition through macrophages in a hypoxic-inflammatory microenvironment. Hepatology 67: 1872–1889 (2018)
66. Zhang Y, Velez-Delgado A, Mathew E, Li D, Mendez FM, Flannagan K, Rhim AD, Simeone DM, Beatty GL, Pasca di Magliano M. Myeloid cells are required for PD-1/PD-L1 checkpoint activation and the establishment of an immunosuppressive environment in pancreatic cancer. Gut 66: 124–136 (2017)
67. Zhu Y, Herndon JM, Sojka DK, Kim KW, Knolhoff BL, Zuo C, Cullinan DR, Luo J, Bearden AR, Lavine KJ, Yokoyama WM, Hawkins WG, Fields RC, Randolph GJ, DeNardo DG. Tissue-Resident Macrophages in Pancreatic Ductal Adenocarcinoma

Originate from Embryonic Hematopoiesis and Promote Tumor Progression. Immunity 47: 263–273 (2017)

Acknowledgments

I would like to say a very big thank you to my supervisor Dr. Milena Armacki for all the support and guidance she gave me. I also would like to thank Prof. Dr. Thomas Seufferlein for providing me with an opportunity to do my doctoral thesis.

I would also like to thank Claudia Ruhland for introducing me to lab work and helping me in numerous ways.

Special thanks go to Dr. Dr. Alpaslan Taşdoğan who convinced me that I should pursue my doctoral degree and helping in whatever way he could during this period.

Last but not least, I would like to express my deepest gratitude to my family and friends for their patience and support.

CV was removed due to data privacy reasons